The Journal of Experimental Biology 202, 1023–1046 (1999)
Printed in Great Britain © The Company of Biologists Limited 1999
JEB1891

IN VIVO LOCOMOTOR STRAIN IN THE HINDLIMB BONES OF *ALLIGATOR MISSISSIPPIENSIS* AND *IGUANA IGUANA*: IMPLICATIONS FOR THE EVOLUTION OF LIMB BONE SAFETY FACTOR AND NON-SPRAWLING LIMB POSTURE

RICHARD W. BLOB[1,*] AND ANDREW A. BIEWENER[2]

[1]*Committee on Evolutionary Biology, University of Chicago, 1027 East 57th Street, Chicago, IL 60637, USA* and *Department of Geology, Field Museum of Natural History, Roosevelt Road at Lake Shore Drive, Chicago, IL 60605, USA* and [2]*Concord Field Station, MCZ, Harvard University, Old Causeway Road, Bedford, MA 01730, USA*

*Present address: Division of Fishes, Department of Zoology, Field Museum of Natural History, Roosevelt Road at Lake Shore Drive, Chicago, IL 60605, USA (e-mail: rblob@fmnh.org)

Accepted 16 February; published on WWW 6 April 1999

Summary

Limb postures of terrestrial tetrapods span a continuum from sprawling to fully upright; however, most experimental investigations of locomotor mechanics have focused on mammals and ground-dwelling birds that employ parasagittal limb kinematics, leaving much of the diversity of tetrapod locomotor mechanics unexplored. This study reports measurements of *in vivo* locomotor strain from the limb bones of lizard (*Iguana iguana*) and crocodilian (*Alligator mississippiensis*) species, animals from previously unsampled phylogenetic lineages with non-parasagittal limb posture and kinematics. Principal strain orientations and shear strain magnitudes indicate that the limb bones of these species experience considerable torsion during locomotion. This contrasts with patterns commonly observed in mammals, but matches predictions from kinematic observations of axial rotation in lizard and crocodilian limbs. Comparisons of locomotor load magnitudes with the mechanical properties of limb bones in *Alligator* and *Iguana* indicate that limb bone safety factors in bending for these species range from 5.5 to 10.8, as much as twice as high as safety factors previously calculated for mammals and birds. Limb bone safety factors in shear (3.9–5.4) for *Alligator* and *Iguana* are also moderately higher than safety factors to yield in bending for birds and mammals. Finally, correlations between limb posture and strain magnitudes in *Alligator* show that at some recording locations limb bone strains can increase during upright locomotion, in contrast to expectations based on size-correlated changes in posture among mammals that limb bone strains should decrease with the use of an upright posture. These data suggest that, in some lineages, strain magnitudes may not have been maintained at constant levels through the evolution of a non-sprawling posture unless the postural change was accompanied by a shift to parasagittal kinematics or by an evolutionary decrease in body size.

Key words: locomotion, biomechanics, bone strain, safety factor, posture, evolution, Sauria, Crocodylia, Lepidosauria, lizard, *Alligator mississippiensis*, *Iguana iguana*.

Introduction

Terrestrial tetrapods have evolved a diverse range of limb postures spanning a continuum from sprawling, in which the limbs are held lateral to the body, to fully upright, in which the limbs are held beneath the body (Jenkins, 1971a; Gatesy, 1991a). Differences in limb posture among species have been correlated with differences in many aspects of locomotor function, ranging from limb bone morphology (Bertram and Biewener, 1990; Gatesy, 1991b) to limb kinematics (Jenkins, 1971a; Gatesy, 1991a; Reilly and DeLancey, 1997a,b; Reilly and Elias, 1998). Yet studies of limb bone loading during locomotion have generally examined only mammalian or avian species in which limb motion is restricted to a parasagittal or nearly parasagittal plane: the consequences of non-parasagittal limb posture and kinematics for limb bone loading have not been investigated. Because upright, parasagittal posture is a derived condition among mammals (Jenkins, 1971a,b) and amniotes in general (Brinkman, 1980a,b, 1981; Gatesy, 1991a), broad extrapolations of skeletal loading patterns from mammals that use parasagittal limb motion to other species that use different limb postures and kinematics are suspect. Such extrapolations potentially oversimplify the functional diversity of loading patterns in tetrapod limbs and mask insights into the evolutionary history of tetrapod locomotor mechanics. To examine the evolution of locomotor mechanics across transitions from sprawling to non-sprawling posture, comparative biomechanical data from non-mammalian species with non-parasagittal kinematics are required.

One approach used to examine limb bone loading mechanics during terrestrial locomotion is *in vivo* measurement of limb bone strains (e.g. Lanyon and Smith, 1970; Rubin and Lanyon,

1982; Biewener et al., 1983, 1988; Biewener and Taylor, 1986). Results from studies of mammalian and avian bone strains have led to two general conclusions. First, tetrapod limb bones supporting the body during terrestrial locomotion are usually loaded in bending or axial compression (Biewener et al., 1983, 1988; Biewener, 1991); torsion is a less common loading regime (Keller and Spengler, 1989; Carrano, 1998). Second, tetrapod limb bones generally have safety factors between 2 and 4 (i.e. are able to withstand 2–4 times the strain they usually incur: Alexander, 1981; Biewener, 1993). However, because available strain data come from a restricted functional and phylogenetic range of animals (mammals and birds with parasagittal or nearly parasagittal limb kinematics), the generality of these conclusions among all amniotes is uncertain. The broader diversity of locomotor strain patterns and their implications for the evolution of skeletal design remain largely unexplored.

This study reports the results of *in vivo* locomotor strain recordings from the femur and tibia of the American alligator (*Alligator mississippiensis*) and the green iguana (*Iguana iguana*), species from the non-parasagittal end of the kinematic continuum and from previously unsampled phylogenetic lineages (Crocodylia and Lepidosauria respectively, *sensu* Brochu, 1997; Gauthier et al., 1988). These data are used to address two fundamental questions. (1) What are the consequences of non-parasagittal locomotion for the mechanics of limb bone loading? (2) What might the mechanics of non-parasagittal locomotion in modern species imply about possible factors in the evolution of non-sprawling posture? To approach these broad questions, we test three more specific hypotheses. First, we test the hypothesis that torsion is a more important mode of limb bone loading during terrestrial locomotion among non-avian saurians (taxonomy *sensu* Gauthier et al., 1988) than among previously examined birds or mammals. Long-axis rotation of the femur and tibia during locomotion in lizards and crocodilians (Brinkman, 1980b, 1981; Gatesy, 1991a) suggests that torsion may predominate in the limb bones of these taxa, in contrast to the dominance of bending and axial compression typical in the limb bones of species with parasagittal limb kinematics (e.g. Biewener, 1983a; Biewener et al., 1983, 1988). Second, we test the hypothesis that the limb bone safety factors of crocodilians and lizards are similar to those observed in birds and mammals. Such similarity might suggest a potential optimal safety factor across all amniotes, regardless of differences in their locomotor function. Finally, we test the hypothesis that limb bone strains will decrease with the use of more upright limb posture by individual animals with the ability to use a range of limb postures. Evolutionary shifts from crouched to upright posture in mammals have been shown to mitigate expected increases in limb bone stress due to size-related increases in limb bone loading (Biewener, 1983a, 1989, 1990). Therefore, lower bone strains might be expected during more upright locomotion by an individual animal that is not incurring increased limb bone loads due to increases in body mass. Because of the wide range of femoral postures employed by *Alligator* (Gatesy, 1991a; Reilly and Elias, 1998), an examination of strain and kinematic data from this species provides an opportunity to test directly the relationship between load magnitude and limb posture within individual animals. By comparing strain data from *Alligator* and *Iguana* with data from previous studies of locomotor strains in birds and mammals, this study seeks to gain insight into mechanical factors potentially influencing the evolution of non-sprawling limb posture.

Materials and methods

Experimental animals and anatomical definitions

Three juvenile *Alligator mississippiensis* (body mass 1.73–2.27 kg, total length 0.98–1.04 m) were provided for strain experiments by the Rockefeller Wildlife Refuge (Grand Chenier, Louisiana, USA). Animals were housed together in a Plexiglas-walled enclosure (245 cm×100 cm×60 cm). Two large plastic cement mixing tubs filled with water were provided as a swimming area for the animals: the water was changed every second day. Temperature was maintained between 29 and 32 °C. Animals were fed a diet of chicken hearts, gizzards and livers mixed with a vitamin/mineral supplement. A 13 h:11 h light:dark cycle and full-spectrum light were provided. The diet supplement and full-spectrum light were supplied to help maintain natural limb bone mass in spite of captivity (Frye, 1995).

Four subadult *Iguana iguana* (body mass 320–516 g, snout–vent length 229–260 mm) were purchased from Glades Herps (Fort Myers, Florida, USA). The animals were housed in an enclosure similar to that used for the alligators, except that the large water tubs were removed and replaced with objects to climb on and hide in (promoting activity and exercise). The same light and temperature conditions were also maintained. Iguanas were supplied with shallow trays of water and fed a diet of assorted vegetables mixed with a vitamin/mineral supplement (Frye, 1995).

Definitions of anatomical orientations of limb element surfaces for both alligators and iguanas are those of Romer (1956). With the femur oriented such that both distal condyles are parallel to the ground, the ventral surface faces down (towards the ground), the dorsal surface faces up (away from the ground), and anterior and posterior are in the directions of protraction and retraction, respectively. In the crus, the tibia is medial to the fibula. The extensor surface of the tibia is defined as anterior, the flexor surface as posterior, the lateral surface as facing towards the fibula, and the medial surface as facing away from the fibula. During locomotion, the femur rotates during limb support such that the anatomical ‘dorsal’ surface shifts anteriorly in an absolute frame of reference and the anatomical ‘anterior’ surface shifts ventrally (Brinkman, 1980b, 1981; Rewcastle, 1980, 1983; Gatesy, 1991a).

Surgical procedures

Strain gauges were attached surgically to the left (alligator) or right (iguana) femur and tibia of each animal, using aseptic technique and following the protocol of Biewener (1992). All

surgical procedures were approved by the Institutional Animal Care and Use Committee of the University of Chicago (protocols 61341 and 61371). Alligators were initially sedated with intramuscular injections of 50 mg kg^{-1} ketamine and 0.5 mg kg^{-1} xylazine, with volumes evenly divided among the three non-surgical limbs. After sedation, the animals were intubated, and surgical anesthesia was induced and maintained by administering Metofane (methoxyfluorane) through a closed-system anesthesia machine with relative control of inhalant concentration (Pitman-Moore, model 970). Anesthesia was induced in iguanas with initial injections of 100 mg kg^{-1} ketamine and 1 mg kg^{-1} xylazine into the muscles at the base of the tail; supplemental doses were administered as required. These doses were larger than typically recommended for lizards (Bennett, 1991; Boyer, 1992), but initially lower doses administered during the first surgery were insufficient to induce a surgical plane of anesthesia. The animals recovered uneventfully from the dosages used.

To expose gauge attachment sites, medial incisions were made through the skin of the leg and thigh at midshaft. The muscles surrounding the bones were separated along fascial planes and retracted to gain access to the bone surfaces. For femoral sites, it was necessary to penetrate a portion of the extensive attachment of the femorotibialis muscle to expose the bone surface and to attach the gauges slightly distal to midshaft to avoid excessive interference with the origin of this muscle. At each site, a 'window' of periosteum was removed to expose the bone cortex. Bone surfaces were lightly scraped with a periosteal elevator, cleaned with ether, and allowed to dry. Gauges were then attached using a self-catalyzing cyanoacrylate adhesive. In the alligators, single-element gauges (type FLG-1-11; Tokyo Sokki Kenkyujo) were attached to the anterior femur and the medial and posterior tibia; rosette gauges (type FRA-1-11) were attached to the dorsal and ventral femur and the anterior tibia (Fig. 1A). In the iguanas, single-element gauges were attached to the anterior, medial and posterior aspects of the tibia and to the dorsal surface of the femur; a rosette gauge was attached to the anterior aspect of the femur (Fig. 1B). Single-element gauges and the central elements of rosette gauges were aligned with the long axis of the bone to which they were attached. Angular deviations from the long axis were measured during post-experimental dissections and accounted for in calculations where required (mean deviation <5 °). Once all gauges were in place, lead wires from the gauges (336 FTE, etched Teflon; Measurements Group) were passed subcutaneously through a small incision posterodorsal to the acetabulum. All incisions were sutured closed, and the lead wires were soldered into a microconnector and secured to the animals by a self-adhesive bandage wrap. These solder connections then were reinforced with epoxy adhesive.

Strain data collection and analysis

After 2–4 days of recovery, strain recordings were made over the following 2–3 days. A shielded cable was plugged into the microconnector to carry strain signals to Vishay conditioning bridge amplifiers (model 2120; Measurements Group). Raw strain signals were sampled through an A/D converter at 100 Hz (alligators) or 250 Hz (iguanas), calibrated, and stored on a computer for analysis. Owing to the length of the lead wires, strain signals were also corrected for lead wire desensitization (+5 % increase in strain magnitude) as recommended by Biewener (1992). For the alligators, strain data were collected predominantly during treadmill exercise, although some locomotion on a 5 m walled trackway was also recorded. Training consisted of six 90 s periods of exercise

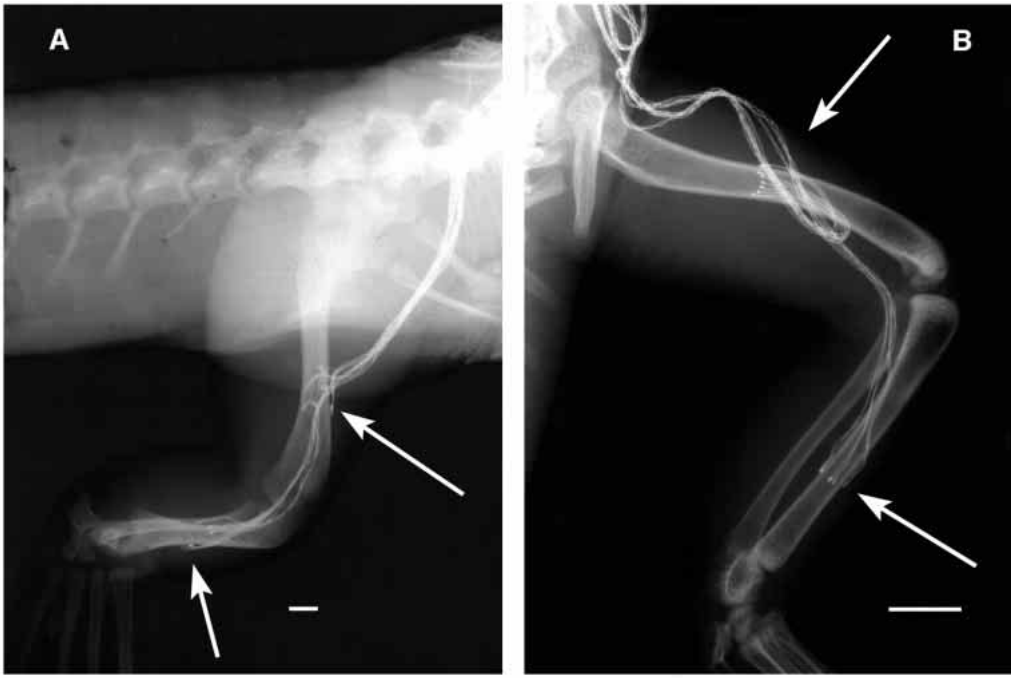

Fig. 1. Radiographs of alligator (*Alligator mississippiensis*) (A) and iguana (*Iguana iguana*) (B) hindlimbs after surgical attachment of strain gauges to the femur and tibia. Gauge locations are indicated by white arrows. Scale bars, 9 mm.

(with periods of rest between), 5 days per week for 3 months. Multiple treadmill trials approximately 40 s in duration were conducted at 0.17 m s^{-1} and 0.37 m s^{-1} for each alligator. The lower speed represented a slow walk for animals of this size (Brinkman, 1980b; Gatesy, 1991a), whereas the faster speed required considerable exertion and was close to the top speed that the animals could sustain. Because the number of data channels from which recordings could be made at the same time was limited, femoral and tibial data were collected during separate trials. For the iguanas, strain data were generated by placing the animals at one end of the 5 m trackway, then startling them by thumping the floor or track walls behind them, causing them to run or walk towards the other end of the track. Multiple trials (with periods of rest between), each recording strains for multiple steps, were conducted for each iguana. Data were collected simultaneously from the femur and tibia. S-VHS (60 Hz) video recordings (Panasonic AG-450) were made of all trials for both species to document locomotor behavior. In the treadmill trials for the alligators, video recordings were obtained from a standard lateral perspective so that kinematic variables and duty factors (the portion of the stride during which the foot contacts the ground) could be calculated. For the iguanas running in the trackway, duty factors were calculated from the strain recordings as the length of time over which a strain peak was present, divided by the length of time from the start of one peak to the start of the following peak. Upon completion of the recordings, the animals were killed (Nembutal sodium pentobarbital, 200 mg kg^{-1} intraperitoneal injection) and stored for later dissection.

Conventions for analysis and interpretation of strain data were as follows. Tensile strains are recorded as positive and compressive strains are negative. The magnitudes of peak longitudinal strain (strain aligned with the axis of the bone) were digitized from each gauge location for each step. The distribution of tensile and compressive strains on the cortex of a bone provides information about the loading regime to which the bone is subjected. For instance, compressive strains at all sites would suggest loading in axial compression, whereas equal magnitudes of tensile and compressive strains on opposite cortices would indicate pure bending; unequal magnitudes of tension and compression on opposite cortices would suggest a combination of axial and bending loads. Magnitudes and orientations of principal strains (maximum and minimum strains at a site, potentially not aligned with the long axis of the bone) were calculated from the rosette gauge data (Dally and Riley, 1978). Shear strains also were calculated following the methods of Carter (1978) and Biewener and Dial (1995). In conjunction with calculations of principal strain orientations, calculations of shear strains allowed evaluation of the importance of torsional loading. Defining the long axis of the bone as 0°, pure torsional loads would show principal strain orientations (deviations from the bone long axis) of +45° or −45°, depending on whether the bone was twisted in a clockwise or counterclockwise direction. Orientations of principal tensile strain (ϕ_t) differing by 180° are equivalent, and orientations of principal tensile and compressive strains are orthogonal.

Following muscular dissections of the hindlimbs of the animals, the instrumented leg bones were excised and embedded in epoxy resin. The bones then were sectioned transversely at the gauge sites using a diamond annular saw (Microslice II; Cambridge Instruments Ltd), and the sections were mounted on glass slides. Using a digitizing tablet, coordinate data were generated from outlines traced from the cross sections, and the locations of the gauges on the bone perimeter were digitized. Following the methods of Carter et al. (1981) and Biewener and Dial (1995), the digitized coordinates of the bone outline and gauge locations, together with strain data from the three separate recording sites for the alligator femur, alligator tibia and iguana tibia were used to calculate the location of the neutral axis of bending (where strain is zero) and the planar distribution of longitudinal strains through cross sections of those elements.

Mechanical property tests

Upon removal of the instrumented leg bones, the intact remains of the iguana and alligator specimens were frozen. Specimens were later thawed, and the femora and tibiae contralateral to the instrumented limbs were excised for measurements of yield and failure strain in bending tests. Care was taken to avoid scratching or damaging bone surfaces during extraction. Soft tissue was cleared from the bone diaphyses by firmly rubbing the surface using a saline-soaked cotton-tipped applicator, although residual ligamentous tissue was allowed to remain on the articular surfaces. Hydration of the bones was maintained with saline solution after the removal of soft tissue. Upon cleaning the bones, exposed surfaces were lightly sanded with 600 grit paper to ensure removal of any surface flaws. Three single-element strain gauges (type FLK-2-11) were then bonded to the bone cortex around the midshaft circumference of each element. For tibiae, anterior, medial and posterior sites were selected; for femora, a dorsal site was selected, as well as two ventral sites, one anterior and one posterior to the ventral muscle scar of the femorotibialis. Attachment sites were cleaned with methyl-ethyl-ketone only, using no additional scraping, and gauges again were bonded with cyanoacrylate adhesive. No gauge orientation deviated by more than 5° from the long axis of a bone.

Whole bone specimens were tested in three-point bending using a Type K (Monsanto) tensometer fitted with a 600 N steel force beam to which a strain gauge had been bonded. The gauge length of the three-point bending jig was 30 mm, yielding a 15 mm bending moment arm (bone lengths ranged from 40 to 57 mm). Bones were positioned in the jig so that the strain gauges bonded to them were at the level of the central point of load. In addition, bones were oriented so that during testing tensile strains would develop on the surfaces on which they developed during the locomotor trials, on the basis of the *in vivo* strain recordings. Thus, femora were positioned to place the ventral surface in tension, whereas tibiae were positioned to place the anterior surface in tension. These

positions placed at least one gauge on each bone (ventroposterior for femora, anterior for tibiae) on a surface where maximum tensile strains would be expected to develop during the tests. Bones were loaded at a constant displacement rate (0.08 mm s^{-1}) until failure. The voltage outputs from the force beam and the gauges bonded to the test bones were collected through bridge amplifiers and an A/D converter and stored on a computer for analysis. For each trial, applied bending moment (applied force multiplied by the bending moment arm) was plotted *versus* maximum tensile strain. Yield strains were then calculated following the protocol of Currey (1990): the slope of the initial, linear portion of the curve was calculated, and the point at which strain magnitude deviated by 200 microstrain (hereafter abbreviated με=strain×10^{-6}) from the magnitude expected on the basis of this slope was considered to be the point of yield.

Safety factors for the hindlimb bones of *Iguana* and *Alligator* were calculated as the ratio of yield strain (following the recommendation of Biewener, 1991) to peak functional strain for each bone in each species (evaluated in the planar strain analyses):

$$\text{Safety factor} = (\text{yield strain}/\text{peak functional strain}) . \quad (1)$$

'Mean' safety factors were calculated from the mean values of peak strains and mechanical properties. In addition, when error ranges were available for yield strains or peak functional strains, 'worst-case' (i.e. lowest possible) safety factors were calculated, on the basis of (mean yield strain minus 2 S.D.) and (mean peak functional strain plus 2 S.D.).

Correlations between strain magnitude and limb posture

To test the correlation between limb posture and strain magnitude in alligators, the angle of midstep femoral adduction was calculated for each femoral strain peak. Strain recordings were synchronized to the kinematic video recordings using a pulse generator that simultaneously flashed a light pulse in the field of view of the video and sent a voltage pulse to the A/D converter. For each footfall during femoral recordings, markers on the knee and hip joints were used to digitize the length of the femur in lateral view when it was perpendicular to the treadmill (Measurement TV; Updegraff, 1990). Midstep femoral adduction angle (γ) then was calculated for each step as:

$$\gamma = 90 - [\cos^{-1} (\text{observed length}/\text{true length})] . \quad (2)$$

True femur lengths were measured directly from the animals, and higher values of γ reflect greater femoral adduction (i.e. a more upright posture). Reduced major axis (RMA) regressions of strain magnitude on γ were calculated for each recording location to evaluate correlations between these variables (for similar treatment of angular kinematic data, see Reilly and DeLancey, 1997b). RMA is the most appropriate method of regression for the evaluation of structural relationships between variables when both are subject to error (LaBarbera, 1989; Sokal and Rohlf, 1995).

Results

Locomotor strain patterns and magnitudes

Representative principal, shear and longitudinal strain traces from the alligator and iguana limb bones are illustrated in Figs 2–5; mean peak strain magnitudes at the different recording locations are summarized in Tables 1–4. Except for traces from the tibia and anterior femur of *Iguana* (Fig. 4), all graphs are drawn to the same scale to facilitate direct comparisons. Detailed results for the femur and tibia of each species are described below. Generalizations about limb bone strains during fast and slow locomotion for each species are made on the basis of the most common strain patterns observed for each recording site, interpreting these patterns as standard behavior. Some repeated, but non-standard, patterns are described in a separate section after these general characterizations.

Fast locomotion in Alligator*: femur*

Representative strain traces from an alligator femur during fast locomotion are illustrated in Fig. 2; mean peak strain magnitudes for each femoral recording site during fast steps are reported in Table 1. Peak strain magnitudes are quite variable (coefficients of variation between 0.39 and 0.80), but

Table 1. *Peak longitudinal (ε_{axial}), principal tensile (ε_t), principal compressive (ε_c) and shear strains recorded from the alligator femur and tibia during fast (0.37 m s^{-1}) locomotion*

Bone	Gauge site	ε_{axial} (με)	ε_t (με)	ε_c (με)	ϕ_t (degrees)*	Shear (με)
Femur	Dorsal	−400±319 (161, 2)	+232±122 (214, 3)	−468±254 (214, 3)	+47±13 (214, 3)	619±306 (214, 3)
	Ventral	+434±190 (76, 1)	+708±273 (76, 1)	−537±221 (76, 1)	+29±13 (76, 1)	1027±591 (76, 1)
	Anterior	+377±162 (176, 3)				
Tibia	Anterior	+231±90 (218, 3)	+391±164 (218, 3)	−361±215 (218, 3)	−35±11 (218, 3)	677±388 (218, 3)
	Medial	+415±197 (230, 2)				
	Posterior	−880±327 (234, 2)				

Values are means ± S.D. (με = 10^{-6} × strain).
Angles of principal tensile strains to the long axis of the bone (ϕ_t) are also reported.
Following strain magnitudes in parentheses are the number of steps analyzed and the number of individuals tested, respectively.
*Rotational directions for ϕ_t: dorsal femur, + = proximoanterior; ventral femur, + = proximoposterior; anterior tibia, – = proximolateral.

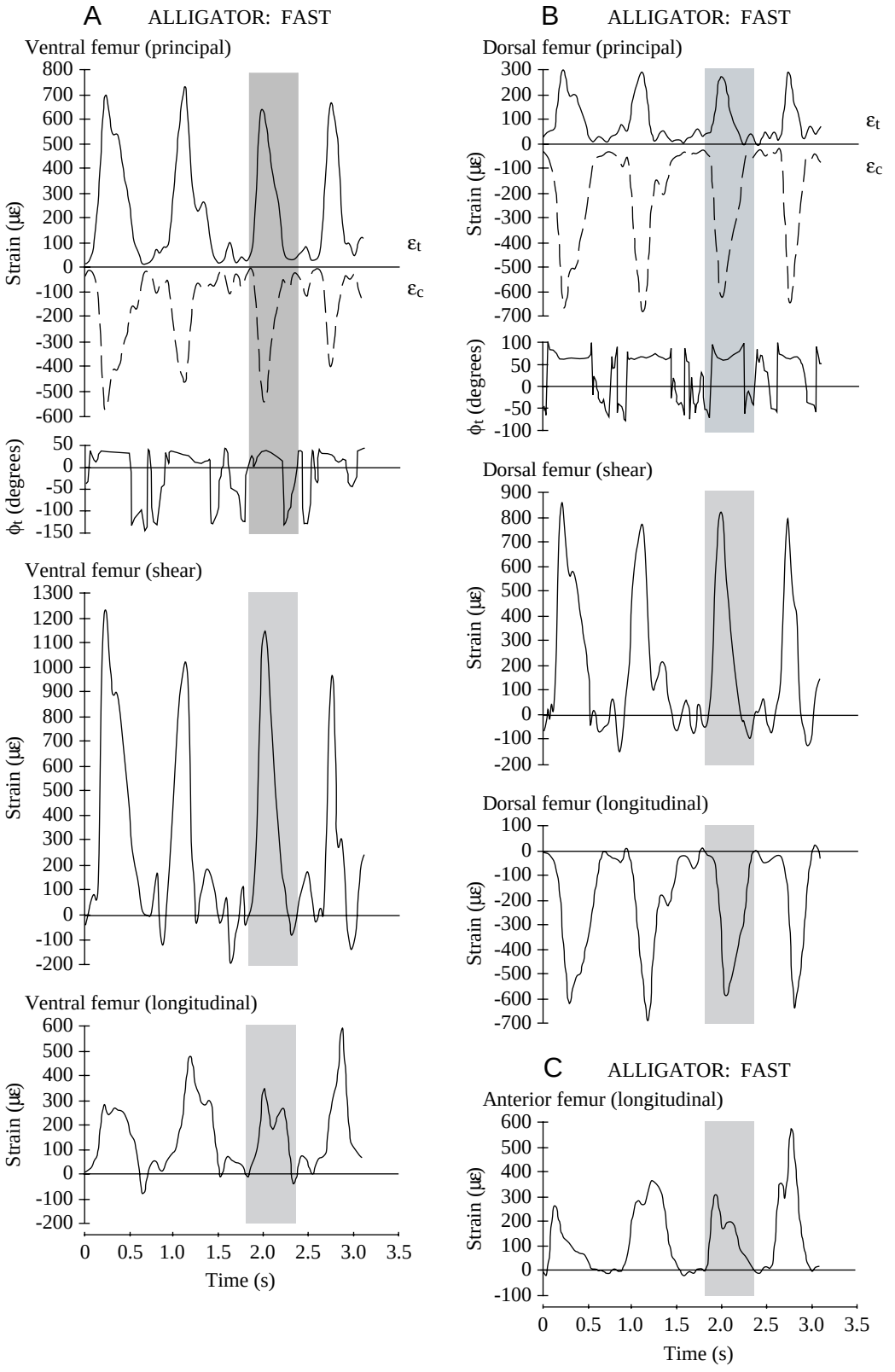

Fig. 2. Representative strain traces recorded simultaneously from the three gauge locations on the alligator femur during fast locomotion ($0.37\,m\,s^{-1}$). Four consecutive steps are illustrated. (A) Ventral principal, shear and longitudinal strain. (B) Dorsal principal, shear and longitudinal strain. (C) Anterior longitudinal strain. Shading highlights the same single step at all gauge locations. ε_t and ε_c denote the tensile and compressive principal strain traces, respectively; compressive principal strain is shown as a dashed line. ϕ_t indicates the angular deviation of principal tensile strains from the long axis of the bone.

loading patterns (i.e. patterns of tensile and compressive strain at each recording site) are consistent among steps. Peak strains at all locations are approximately synchronous and typically occur slightly before midstep. Longitudinal strain traces often exhibit two peaks per step, reflecting the initial deceleration of the animal upon contact of the foot with the ground, followed by the reacceleration of the animal when the foot pushes off from the ground (Alexander, 1977a). However, ventral and dorsal principal strain traces often show only single peaks, consistent with the pattern seen during faster locomotion in previous studies of mammalian limb bone strains (e.g. Lanyon and Bourn, 1979; Rubin and Lanyon, 1982; Biewener and Taylor, 1986; Biewener et al., 1988).

The distributions and relative magnitudes of tensile and compressive strains indicate that the alligator femur is subject to a combination of bending, axial compression and torsion. Anterior and ventral aspects of the alligator femur experience tension: longitudinal strains are positive on both surfaces, and ventral principal tensile strains are larger than ventral principal compressive strains (Table 1; Fig. 2A,C). Mean peak strains recorded from these sites were +708 με (ventral, principal) and +377 με (anterior, longitudinal). In contrast, the dorsal surface of the femur experiences compression: longitudinal strains are compressive, and compressive principal strains are greater than tensile principal strains (mean peak principal strain −468 με; Fig. 2B; Table 1). The presence of tensile and compressive strains on opposite bone surfaces suggests that the alligator femur is loaded in bending. In addition, because dorsal compressive longitudinal strains are greater in absolute magnitude than ventral tensile longitudinal strains during single steps in which recordings were taken from both locations (Fig. 2A,B), bending loads appear to be superimposed on axial compression induced by supporting the weight of the body. However, mean peak principal tensile strain orientations (ϕ_t) on the dorsal (+47 °, proximoanterior) and ventral (+29 °, proximoposterior) femoral surfaces deviate strongly from the long axis of the bone, suggesting that the alligator femur also experiences torsion (Table 1; Fig. 2). The direction of torsion (clockwise for the left femur viewed from its proximal or distal end) is consistent with the direction of stance phase femoral rotation observed in cineradiographic studies of crocodilian locomotion (Brinkman, 1980b; Gatesy, 1991a): anterior femoral rotation is produced by the caudofemoralis muscle, which inserts proximally on the femur (Gatesy, 1997), but femoral rotation is resisted distally by the ligaments of the knee joint. Shear strain magnitudes further suggest that the alligator femur experiences substantial torsion: mean peak dorsal (619 με) and ventral (1027 με) femoral shear strains exceed mean peak femoral principal strain measurements from these sites by 32 % and 45 % respectively (Table 1; Fig. 2A,B).

Fast locomotion in Alligator*: tibia*

Representative strain traces from an alligator tibia during fast locomotion are illustrated for four sequential steps in Fig. 3A, and mean peak strain magnitudes for each tibial recording site during fast steps are reported in Table 1. Loading patterns are consistent among steps, although load magnitudes are variable (coefficients of variation between 0.39 and 0.57). All longitudinal traces and most principal strain traces exhibit two peaks, one before and one after midstep.

The alligator tibia, like the alligator femur, is loaded in a combination of bending, axial compression and torsion. Longitudinal recordings show that, through the first half of stance, the anterior and medial aspects of the tibia are loaded in tension, whereas the posterior surface is loaded in compression (Fig. 3A). After midstep, loading patterns are unchanged for the anterior and posterior surfaces, but medial longitudinal strains shift from tensile to compressive. Nonetheless, the presence of both tensile and compressive surface strains and the greater magnitude of posterior compression (mean −880 με) compared with anterior (mean +231 με) or medial (mean +415 με) tension suggest that bending is superimposed on axial compression in the tibia. The deviation of peak principal tensile strains from the long axis of the tibia on its anterior surface (mean ϕ_t −35 °, proximolateral; Table 1) suggests that the alligator tibia is also loaded in torsion. This torsion is counterclockwise for the left tibia (viewed from its proximal or distal end), consistent with cineradiographic observations of outward crural rotation during locomotion in *Caiman sclerops* (Brinkman, 1980b) resisted by the foot (planted on the ground) and the ligaments of the ankle. Shear strain calculations reflect the likely importance of torsion in the tibia: mean peak anterior shear strain (677 με) exceeds mean peak anterior principal tensile strain (+391 με) by 73 % (Table 1; Fig. 3A).

Slow locomotion in Alligator*: femur and tibia*

Except for ventral longitudinal strains, all longitudinal, principal and shear strains in the femur decrease significantly in magnitude during slow locomotion compared with fast locomotion (Tables 1, 2; compare dorsal, ventral and anterior recording locations: Mann–Whitney *U*-tests, $P<0.01$ for all comparisons). However, at some locations, these differences are fairly minor (e.g. <50 με for dorsal principal tensile strains). Mean peak strain magnitudes for the femur are still variable during slower locomotion (coefficients of variation between 0.26 and 0.60), but the distribution of tensile and compressive strains is essentially the same during fast and slow steps.

In the tibia, anterior principal tensile and compressive strains are both significantly lower in slow steps, as are anterior and posterior longitudinal strains (compare Table 1 with Table 2; Mann–Whitney *U*-tests, $P<0.05$ for anterior principal compressive strain, $P<0.002$ for other comparisons). However, mean peak strains at the medial recording site increase significantly during slower locomotion (Mann–Whitney *U*-test, $P<0.001$; Table 1); in addition, medial strains remain tensile throughout the stance phase at slow speed and no longer exhibit the compressive peak seen at the end of the support phase in fast steps (Fig. 3B). Torsion remains important during slow steps. Deviations of principal tensile strains from the long

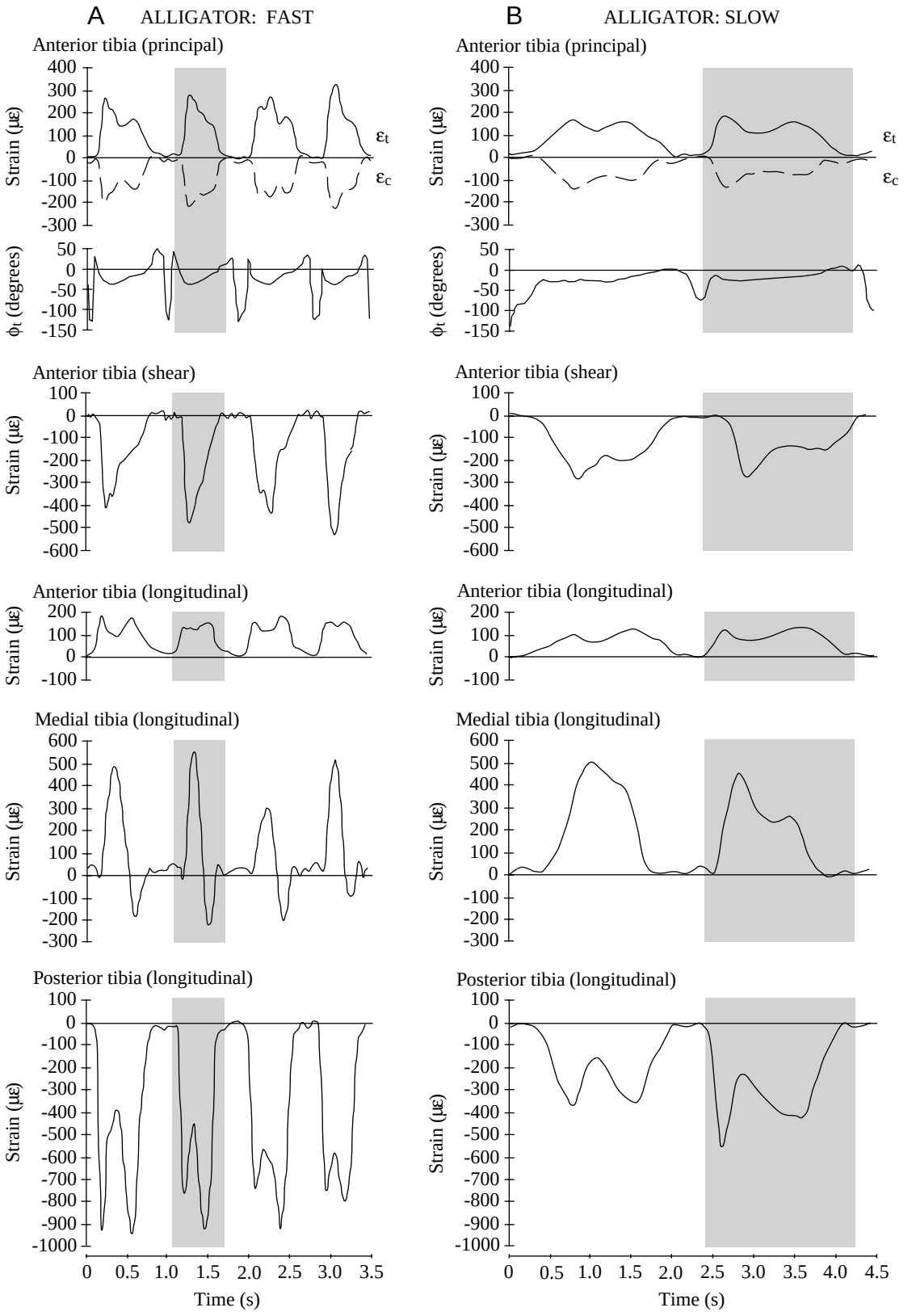

Fig. 3. Representative principal, shear and longitudinal strain traces recorded simultaneously from the three gauge locations on the alligator tibia. (A) Fast locomotion ($0.37\,m\,s^{-1}$) showing four consecutive steps. (B) Slow locomotion ($0.17\,m\,s^{-1}$) showing two consecutive steps. Symbols and format as in Fig. 2.

Table 2. *Peak longitudinal, principal and shear strains recorded from the alligator femur and tibia during slow (0.17 m s^{-1}) locomotion*

Bone	Gauge site	ε_{axial} (με)	ε_t (με)	ε_c (με)	ϕ_t (degrees)*	Shear (με)
Femur	Dorsal	–197±119 (67, 2)	+187±57 (99, 3)	–349±89 (99, 3)	+42±12 (99, 3)	493±139 (99, 3)
	Ventral	+235±85 (23, 1)	+340±123 (23, 1)	–257±99 (23, 1)	+28±10 (23, 1)	474±243 (23, 1)
	Anterior	+259±138 (111, 3)				
Tibia	Anterior	+198±91 (131, 3)	+342±151 (131, 3)	–323±173 (131, 3)	–36±11 (131, 3)	617±333 (131, 3)
	Medial	+512±134 (111, 2)				
	Posterior	–465±153 (129, 3)				

Values are means ± S.D.
Format and abbreviations are as in Table 1.
*Rotational directions for ϕ_t are the same as those used in Table 1.

axis of the tibia are virtually identical in slow and fast steps (mean ϕ_t –36° and –35° for slow and fast steps, respectively; Tables 1, 2), and mean peak anterior shear strain (617 με) still exceeds mean peak anterior principal tensile strain (+342 με) by 80% during slow locomotion (Table 2; Fig. 3B).

Fast locomotion in Iguana*: femur*

Running steps (mean velocity 2.0 m s^{-1}) were elicited from two of the four experimental iguanas (iguanas B and D). Representative principal and axial strain traces for iguana B are illustrated in Fig. 4A, and representative principal and shear traces for iguana D are illustrated in Fig. 5A; mean peak strain magnitudes for both animals are listed in Table 3. The iguana femur, like the alligator femur, appears to be loaded in bending with the anterior cortex in tension and the dorsal cortex in compression (Fig. 4A; Table 3). However, patterns of femoral torsion differed among the individual iguanas. In iguana B (*N*=45 steps), anterior principal tensile strains were aligned very closely with the long axis of the femur (mean ϕ_t –3°, proximoventral), and femoral shear strains were negligible (Fig. 4A; Table 3). In contrast, in iguana D (*N*=7 steps), ϕ_t deviated considerably from the long axis of the femur at peak strain (mean –49°, proximoventral; Fig. 5A), resulting in anterior shear strains 78% greater than anterior principal tensile strains (mean peak shear 1121 με, mean peak anterior principal strain +629 με; Table 3). Thus, torsion appears to be unimportant for the femur of iguana B, but large shear and off-axis principal strains suggest considerable torsion in the femur of iguana D. The counterclockwise torsion measured on the right femur of iguana D is consistent with the clockwise torsion measured on the left femur of alligators, as patterns of torsion in contralateral limbs would be expected to mirror each other. Furthermore, the direction of torsion in iguana D is consistent with the direction of stance phase femoral rotation observed in previous cineradiography of iguana locomotion (Brinkman, 1981): anterior femoral rotation is produced by the caudofemoralis, which inserts proximally on the femur (Snyder, 1962), but rotation is resisted distally by the ligaments of the knee.

Fast locomotion in Iguana*: tibia*

Strain patterns for the tibia were similar among the individual iguanas (Fig. 4B). Longitudinal strain traces show single peaks with synchronous maxima at approximately midstep. Like the alligator tibia, the iguana tibia is subject to bending: the anterior and medial tibial surfaces experience tensile strains (mean peaks +1650 με and +982 με, respectively), whereas the posterior surface experiences compressive strains (mean peak –840 με). The greater magnitude of anterior tensile strains relative to posterior compressive strains suggests that the iguana tibia is loaded in net tension. This result is unexpected for a limb element

Table 3. *Peak longitudinal, principal and shear strains recorded from the iguana femur and tibia during running steps*

Bone	Gauge site	Individual(s)	ε_{axial} (με)	ε_t (με)	ε_c (με)	ϕ_t (degrees)*	Shear (με)
Femur	Anterior	Iguana B	+288±130 (45, 1)	+291±128 (45, 1)	–308±122 (45, 1)	–3±5 (45, 1)	59±73 (45, 1)
	Anterior	Iguana D	–235±78 (7, 1)	+629±94 (7, 1)	–510±85 (7, 1)	–49±4 (7, 1)	1121±151 (7, 1)
	Dorsal	Iguana B	–159±42 (45, 1)				
Tibia	Anterior	Both	+1650±608 (49, 2)				
	Medial	Both	+982±328 (52, 2)				
	Posterior	Both	–840±416 (52, 2)				

Values are means ± S.D.
Abbreviations are as in Table 1.
Separate femoral data are reported for the two individuals that exhibited different patterns of femoral shear (see text).
*Rotational direction for ϕ_t: – = proximoventral.

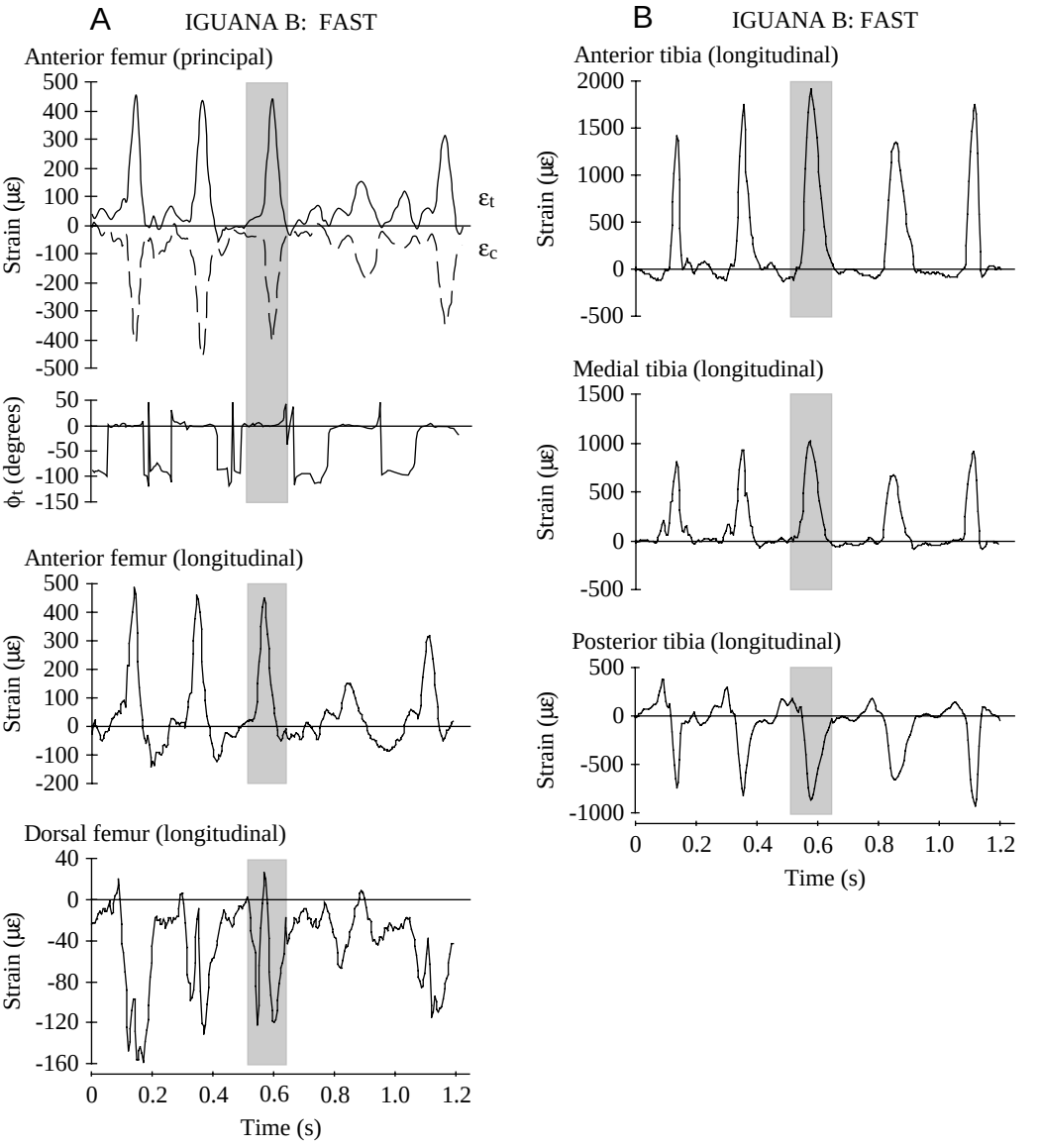

Fig. 4. Representative strain traces recorded simultaneously from the femur and tibia during five consecutive running steps by iguana B. (A) Femoral gauge sites. (B) Tibial gauge sites. Symbols and format as in Fig. 2.

supporting the weight of the body and is explored further through cross-sectional analyses of planar strain distributions (see below). Torsion could not be assessed for the iguana tibia because the cortical surfaces were too narrow to attach rosette gauges.

Slow locomotion in Iguana*: femur and tibia*

Loading patterns for the iguana femur during slow locomotion show some differences from those during fast locomotion. Anterior principal strain traces typically showed double peaks during stance in walking steps, contrasting with the single anterior principal peaks typical of running steps (compare Fig. 5A and 5B). Steps were nearly evenly divided between those in which the first peak (*N*=118) or the second peak (*N*=119) was greater in magnitude (Table 4), as might be expected for normal variation in relative components of deceleration *versus* reacceleration produced by the limb during stance. Principal tensile strain orientations also showed different patterns between walking and running steps. For running steps by iguana D, ϕ_t ranged almost exclusively between 0 ° and –90 °; however, for walking steps, ϕ_t shifted through nearly 180 ° during each step (Fig. 5B). As a result, mean ϕ_t orientations at peak strain were –41 ° for walking steps in which the first strain peak was greater in magnitude, but +18 ° for walking steps in which the second strain peak was greater in magnitude (Table 4). This is consistent with a shift from counterclockwise to clockwise femoral torsion at midstep (viewing the right femur from its proximal or distal end).

Walking steps show the same distributions of tensile and compressive strains as running steps in the iguana tibia: the anterior surface experiences the highest tensile magnitudes, the medial surface experiences relatively lower tensile magnitudes, and the posterior surface remains in compression (Table 4). Mean strain magnitudes at all tibial locations are significantly lower during walking steps than during running

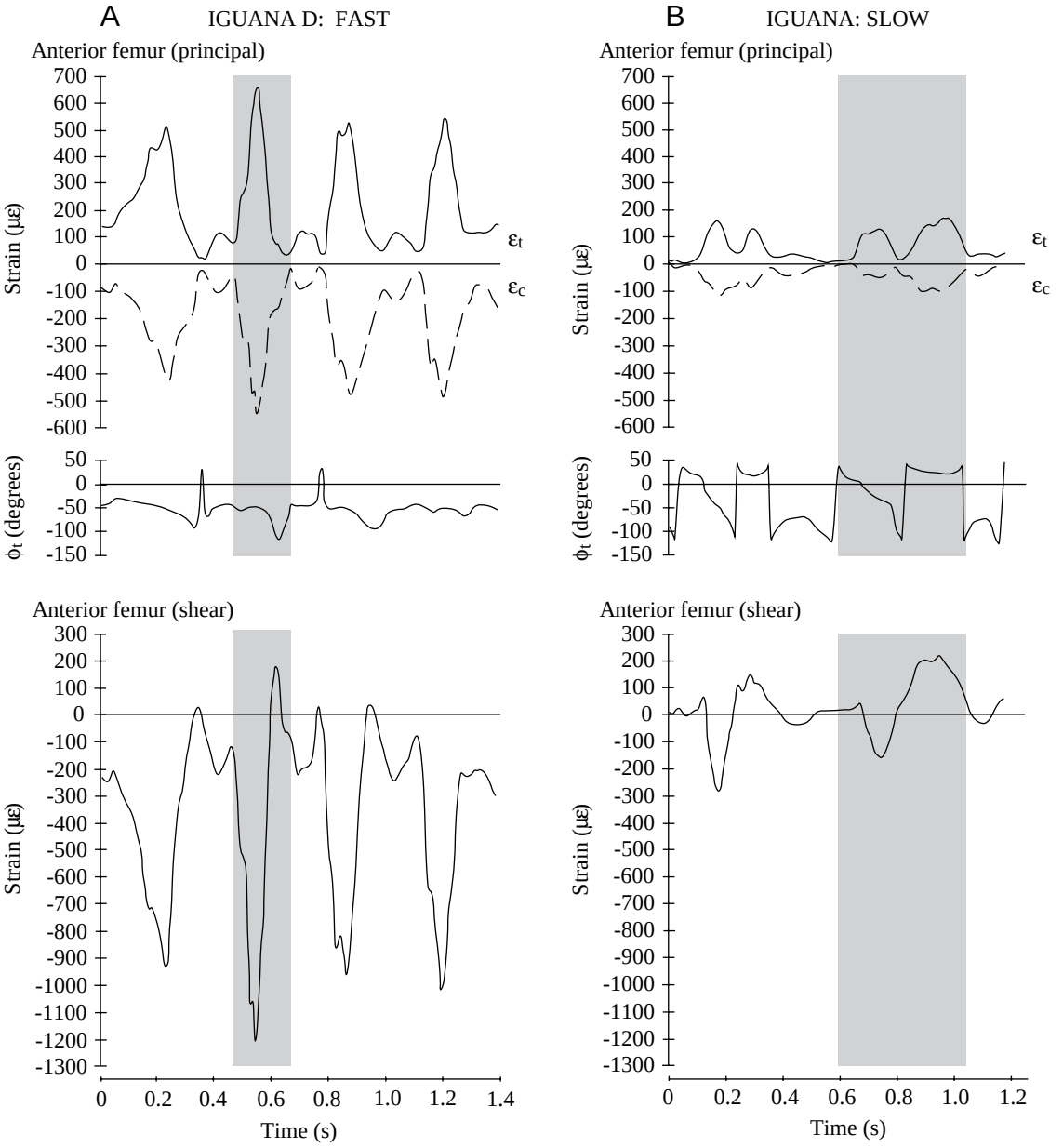

Fig. 5. (A) Representative principal and shear strain traces from the anterior femur of iguana D during four consecutive running steps. (B) Representative principal and shear strain traces from the anterior femur of *Iguana* during two consecutive walking steps. Symbols and format as in Fig. 2.

steps (compare pooled data for tibia in Tables 3 and 4; Mann–Whitney *U*-tests, $P \leqslant 0.005$).

Non-standard patterns and behaviors

In addition to the interindividual variation in femoral strains observed for running by iguanas, other less common, but repeatable, patterns and behaviors were also observed. Although principal strain traces from the alligator femur usually showed a single peak per step, and principal strain traces from the alligator tibia usually had first peaks much greater in magnitude than second peaks, femoral or tibial traces with large second peaks were occasionally evident. In these steps, the sign of ϕ_t was reversed, suggesting that, as in the iguana femur, the direction of bone torsion was reversed during the second half of stance. These steps generally showed the same patterns of axial and principal strains as standard steps and did not consistently exhibit significantly higher or lower mean peak principal or axial strain magnitudes.

During a femoral recording session in the trackway, one alligator darted to the end of the trackway and attempted to climb out, quickly pushing its snout up the wall and raising its trunk off the ground until it was standing on its hindlimbs. It then jumped alternately off each hindlimb several times, so that the body (except for much of the tail) was supported on a single leg during landings. Peak dorsal principal strains recorded from the alligator during jumps (N=5) averaged +566±151 με

Table 4. *Peak longitudinal, principal and shear strains recorded from the iguana femur and tibia during walking steps*

Bone	Gauge site	High rosette peak	ε_{axial} (με)	ε_t (με)	ε_c (με)	ϕ_t (degrees)*	Shear (με)
Femur	Dorsal	First	+163±89 (118, 3)	+360±220 (118, 3)	−285±131 (118, 3)	−41±17 (118, 3)	545±357 (118, 3)
		Second	+227±111 (119, 3)	+273±118 (119, 3)	−218±105 (119, 3)	+18±12 (119, 3)	245±194 (119, 3)
		Pooled	+195±106 (237, 3)	+316±181 (237, 3)	−251±123 (237, 3)	‡	‡
	Anterior	First	−312±145 (62, 1)				
		Second	−241±71 (67, 1)				
		Pooled	−275±118 (129, 1)				
Tibia	Anterior	Pooled	+765±364 (106, 2)				
	Medial	Pooled	+385±178 (237, 3)				
	Posterior	Pooled	−662±313 (237, 3)				

Values are means ± S.D.

Abbreviations are as in Table 1.

For femoral strains, separate means and pooled means are reported for steps in which the first femoral principal strain peak was highest and steps in which the second peak was highest.

*Rotational direction for ϕ_t: − = proximoventral.

‡ϕ_t and shear strains cannot be meaningfully pooled across the two directions of rotation.

(tensile) and −821±225 με (compressive), as much as twice the mean peak strains recorded from this location during fast treadmill locomotion (+232±122 με and −468±254 με, respectively; Fig. 6; means ± S.D.).

Cross-sectional planar strain distributions

Shifts in neutral axis orientation during limb support obtained from cross-sectional analyses of the planar distribution of longitudinal strains are summarized in Fig. 7 for the alligator femur and tibia, as well as the iguana tibia (a similar analysis of the iguana femur was precluded because strain data were available for only two sites). Graphs of cross-sectional strain distributions are compared for the alligator femur and tibia in Fig. 8 and for the iguana tibia in Fig. 9.

In the alligator femur, at the beginning of the step, the neutral axis of bending (NA) is closely aligned with the anteroposterior axis of the bone but displaced ventrally from the cross-sectional centroid (Figs 7, 8A; time 1), causing the

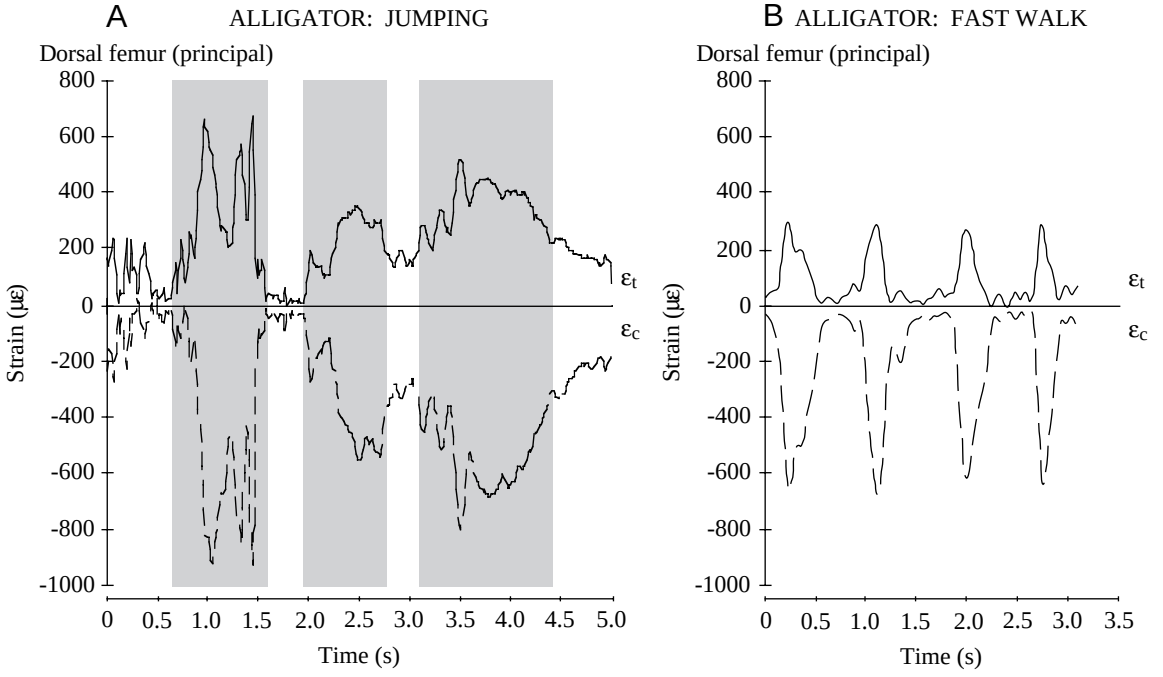

Fig. 6. (A) Principal strain traces from the dorsal femur of *Alligator mississippiensis* during three jumps. Shading indicates periods of foot contact with the ground. (B) Strain traces from the same recording location during normal fast walking steps (0.37 m s^{-1}). Symbols and format as in Fig. 2.

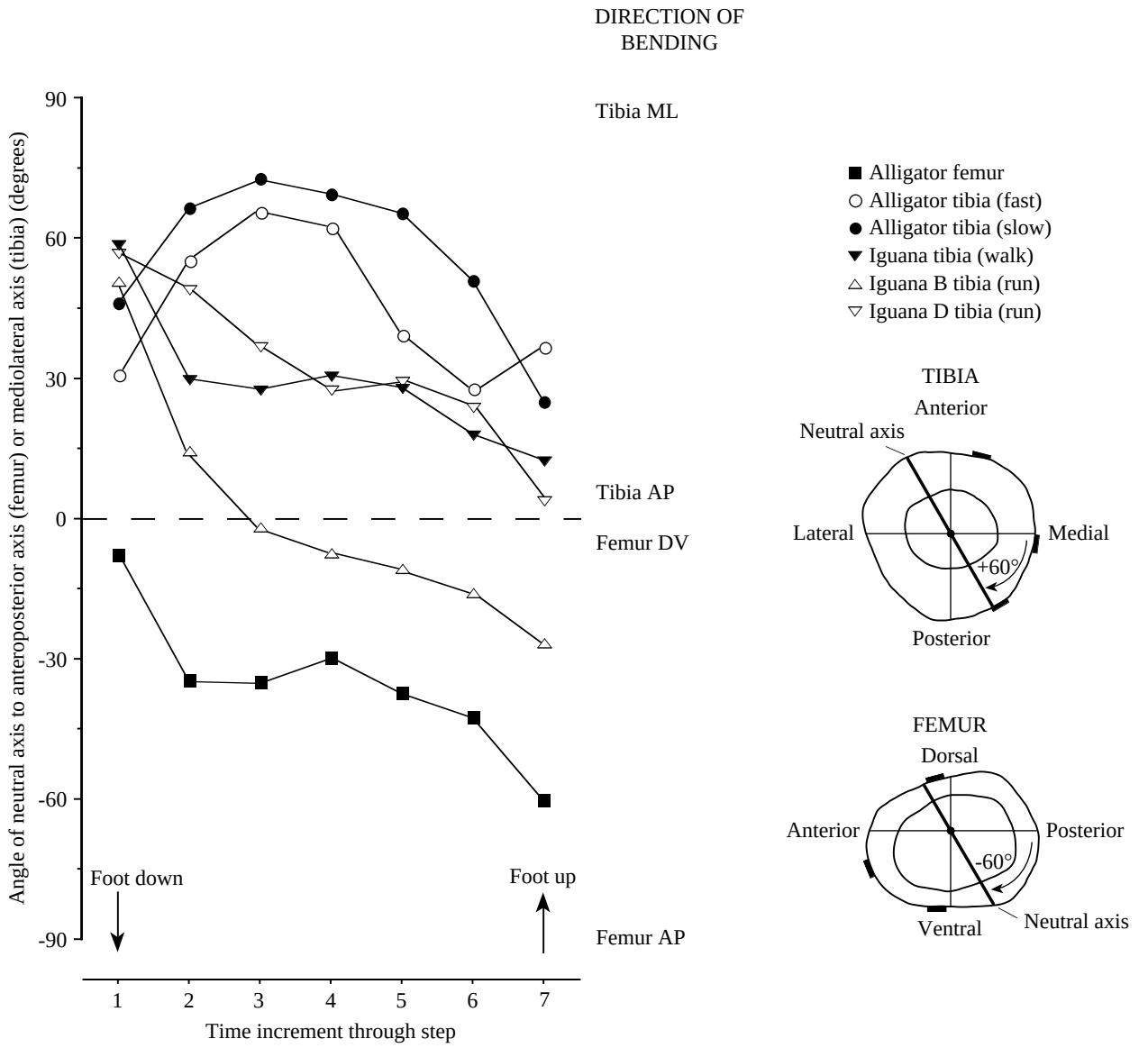

Fig. 7. Shifts in orientation of the neutral axis of bending through the course of stance in the alligator femur and tibia and the iguana tibia averaged from multiple steps (*N*=2–5). Patterns for the alligator tibia during fast and slow locomotion are plotted separately, as are patterns for the iguana tibia during walking and for running by the two individuals (iguanas B and D) with different degrees of femoral torsion (see text). Divisions along the time axis represent equal temporal fractions of each step. Vertical arrows indicate the beginning and end of the stance phase. Schematic bone cross sections to the right of the graph illustrate neutral axis orientations of +60 ° for the tibia and –60 ° for the femur. Strain gauge locations are indicated by the black bars around the cortex of each section. Directions of bending are indicated with respect to the anatomical axes of the bones described in the Materials and methods section, not to an absolute frame of reference. AP, anteroposterior; DV, dorsoventral; ML, mediolateral.

dorsal cortex to be loaded in compression and the ventral cortex in tension. As strain levels increase through the step, the neutral axis shifts towards the centroid and rotates to an anterodorsal/posteroventral direction (–30 ° to –40 °) for most of the remainder of stance. In the context of our principal strain orientation data and the kinematic observations of Brinkman (1980b) and Gatesy (1991a), these changes in NA orientation are consistent with the maintenance of dorsoventral bending (in an absolute frame of reference) through the course of anterior femoral rotation. The displacement of the neutral axis from the centroid and the extent of compressive strains across the femoral cortex confirm axial compression in addition to bending and torsion of the alligator femur. Because peak tensile strains occur at the anteroventral cortex and peak compressive strains at the posterodorsal cortex, rather than at the locations from which strains were recorded on the femur (dorsal, ventral and anterior), peak strains in the alligator femur are probably 35–45 % greater than those measured.

In the alligator tibia, the anteromedial cortex is loaded in tension and the posterolateral surface in compression when the

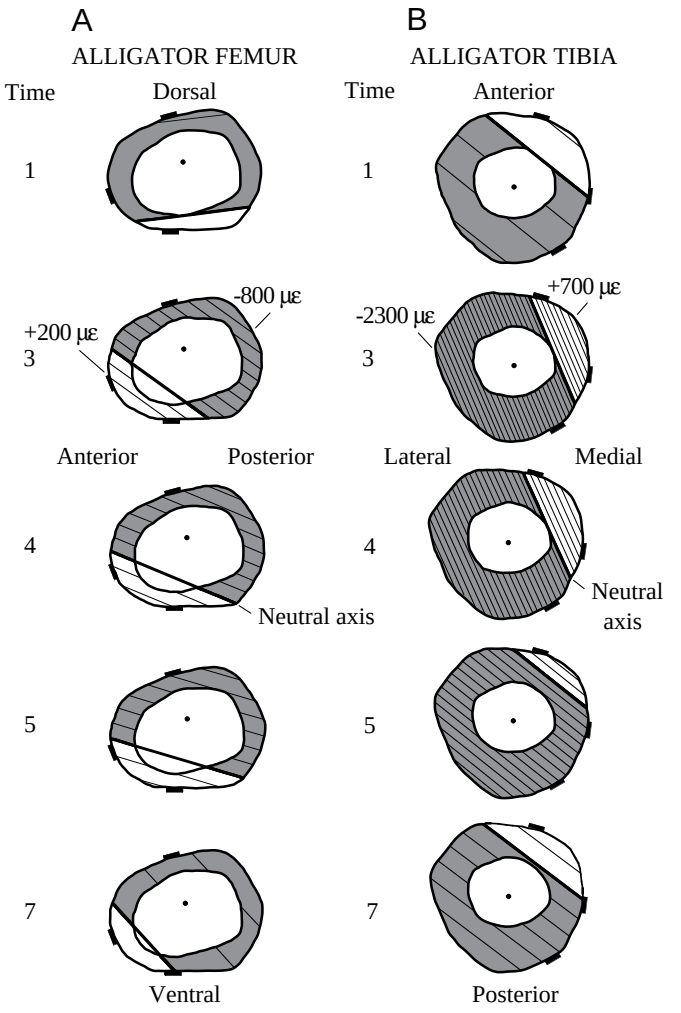

Fig. 8. Graphical comparisons of cross-sectional planar strain distributions calculated for key time increments during representative fast steps for the alligator femur (A) and the alligator tibia (B). Time increment labels correspond to those plotted in Fig. 7 (increments 2 and 6 are not shown). The centroid of each section is indicated by the black dot. Thin lines indicate contours of strain magnitude (all spaced at 100 με). Peak strains calculated for these steps are labeled on the sections at time 3. Compressive strains are shaded. The neutral axis of bending (where strain is zero) is indicated by the boldface strain contour separating compressive and tensile strains (the shaded and non-shaded portions of each plot, respectively); this is labeled for time 4. Black bars on the outer walls of the sections indicate recording locations for strain gauges. Labeled anatomical directions are with respect to the axes described in the Materials and methods section, not to an absolute frame of reference.

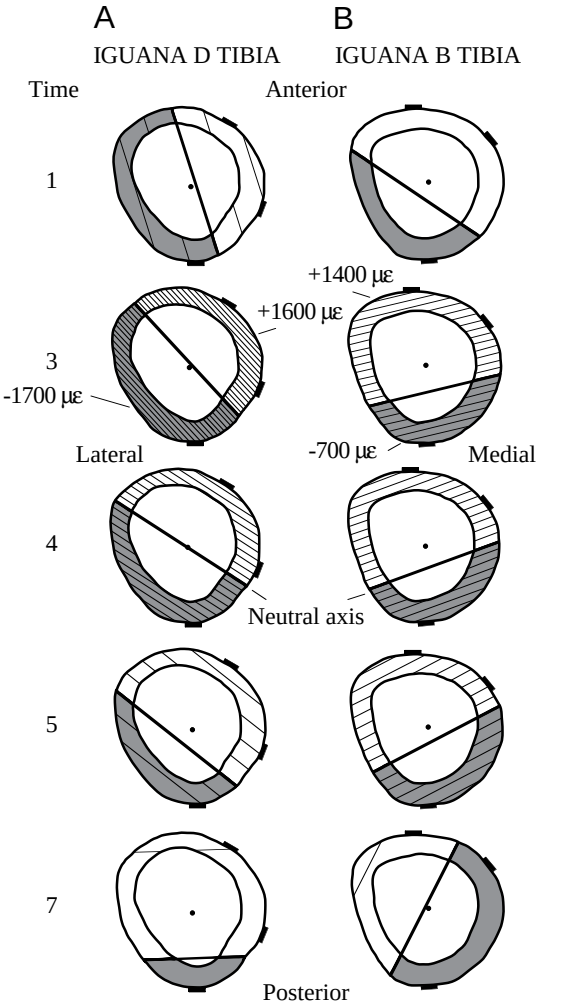

Fig. 9. Graphical comparisons of cross-sectional planar strain distributions calculated for key time increments during representative fast steps for the tibia of iguana D (A) and iguana B (B). Format and symbols as in Fig. 8.

foot contacts the ground; the neutral axis is displaced far from the cross-sectional centroid (Fig. 8B; time 1). Through midstep (Figs 7, 8B; times 2–4), NA orientation shifts more steeply towards the anatomical anteroposterior axis of the bone cross section. In the context of the observed anterior principal strain orientations and Brinkman's (1980b) kinematic data, this shift suggests that tibial bending remains aligned with the direction of travel (anteroposterior, in an absolute frame of reference), even as the bone rotates laterally through the step. During fast steps, NA orientation shifts back towards the mediolateral axis of the tibia soon after midstep and moves further from the centroid, crossing the medial gauge site to place this portion of the cortex in compression (Figs 7, 8B; times 5–7). A similar shift in NA orientation occurs during slow locomotion (Fig. 7), but the medial site does not experience compression because the NA remains closer to the tibial centroid. Because of its orientation and its displacement from the tibial centroid, at peak strain, the neutral axis is shifted quite near the recording sites for the tibial gauges; as a result, peak strain magnitudes during fast steps are probably 2–3 times greater than those recorded.

Planar strain analyses of the tibia were conducted for running steps obtained from each of the iguanas exhibiting the two patterns of femoral torsion. In the animal exhibiting pronounced torsion (iguana D), NA alignment is similar to that in the alligator tibia at the beginning of stance (anterolateral to posteromedial, 55° from the mediolateral axis), but the NA crosses the bone section much closer to the tibial centroid (Figs

7, 9A; time 1). Initially anterior to the centroid, the neutral axis shifts posteriorly through the step, placing the tibia in net axial tension for much of step duration (Fig. 9A; times 4–7). NA orientation also rotates during the step, but in the opposite direction to that observed in alligators. This is consistent with Brinkman's (1980b, 1981) observations that initial rotation of the crus in *Iguana iguana* is opposite in direction to that in *Caiman sclerops*. These changes in NA orientation suggest that, despite differences in the initial direction of tibial rotation in lizards and crocodilians, the direction of tibial bending is correlated with the direction of travel in both species (anteroposterior in an absolute frame of reference). At peak strain, the anterior gauge is close to the site of maximum tensile strain predicted by planar strain analysis; however, planar strain calculations of maximum compressive strains are 50 % greater than those measured at the posterior recording site. The pattern exhibited during walking steps is similar (Fig. 7), except that the neutral axis shifts anteriorly by the end of the step, indicating a return of net axial compression.

Iguana B, which exhibited little torsion during running steps, shows a different pattern of NA orientations in the tibia (Figs 7, 9B). The neutral axis often begins the step posterior to the centroid, indicating net tension relatively earlier than in iguana D (Fig. 9B; time 1). Soon after the foot contacts the ground and throughout most of the remainder of the step, the NA is aligned close to the bone's mediolateral axis (Fig. 9B; times 2–4). By the end of stance, the NA shifts anteriorly past the centroid and the tibia is again loaded in net compression (Fig. 9B; time 7). The anterior and posterior recording sites are both close to the locations of maximum strain predicted from planar strain calculations: predicted maxima exceed measured strains by less than 5 % at both locations. Differences in tibial NA orientation between iguanas B and D correlate with differences in the degree of femoral torsion they experience: iguana D, which experiences greater femoral torsion, also appears to experience greater tibial rotation relative to the direction of travel. However, despite these differences, in both iguanas, the tibia experiences net axial tension for a substantial portion of the step.

Three-point bending tests and safety factor calculations

Catastrophic fracture occurred on the tensile surface in all limb bone specimens tested (Burstein et al., 1972; Currey and Brear, 1974). A representative plot of applied bending moment *versus* maximum recorded tensile strain is illustrated in Fig. 10; the results from all three-point bending tests are summarized in Table 5. Mean fracture strain from eight iguana limb bones (four tibiae, four femora) was +13 449 με (coefficient of variation 26 % of mean); mean yield strain from six specimens (excluding two that fell more than two standard deviations from the mean yield strain) was +9820 με (coefficient of variation 6 % of mean). Yield and fracture strains did not differ significantly between femora and tibiae (P>0.23 for both comparisons; Table 5). One alligator femur also was tested successfully: a fracture strain of +13 366 με and a yield strain of +6495 με were obtained (Table 5).

Prior to safety factor calculations, the mean peak tensile and shear strains measured during locomotion (i.e. peak functional strains; equation 1) were increased by 5 % for the iguana tibia, increased by 45 % for the iguana and alligator femora and multiplied by 3.0 for the alligator tibia to reflect the likely maximal strains indicated by the planar strain analyses (Table 6). Using values of +9820 με for yield strain in iguana bones and +6495 με for yield strain in alligator bones, 'mean' safety factors for bending range from 5.5 (alligator tibia) to 10.8 (iguana femur), and 'worst-case' safety factors range between 3.6 (iguana tibia) and 8.2 (iguana femur) (Table 6). Safety factors for shear are much lower. Assuming that bone will fail in shear at 8000 με (Currey, 1984), mean shear-based safety factors range from 3.9 (alligator tibia) to 5.4 (alligator femur), and 'worst-case' safety factors range between 2.7 (alligator tibia) and 4.3 (iguana femur) (Table 6).

Table 5. *Results of three-point bending tests for* Iguana iguana *and* Alligator mississippiensis *hind limb bones*

Species	Bone	Yield strain (με)	Fracture strain (με)
Iguana	Femur	9819±611 (3)	14749±3099 (4)
	Tibia	9821±645 (3)	12149±3164 (4)
	Pooled	9820±562 (6)	13449±3215 (8)
Alligator	Femur	6495 (1)	13366 (1)

Values are means ± S.D. (in με).
The number of bones per sample is given in parentheses.

Correlation of strain magnitude with femoral posture in Alligator

Regressions for recording locations in two of the three alligators show significant (P<0.05) changes in strain magnitude as femoral posture varies, although correlations are generally weak (r^2<0.35; Fig. 11; Table 7). Strains do not change uniformly across the cortex of the femur as an individual alligator shifts from a sprawling to an upright posture: anterior longitudinal strains decrease as a more upright posture is adopted, whereas dorsal and ventral principal and shear strains appear to increase (Table 7). However,

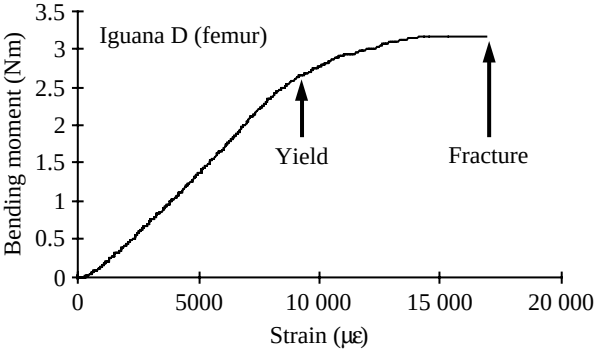

Fig. 10. Representative plot of applied bending moment *versus* maximum tensile strain for a three-point bending test of an iguana femur. Points of specimen yield and fracture are indicated by vertical arrows.

Table 6. *Estimated actual peak locomotor strains and safety factors in* Iguana iguana *and* Alligator mississippiensis *hindlimb bones*

Species	Bone	Factorial increase in strain	Peak calculated tensile bending strain (με)	'Mean' safety factor (bending)	'Worst-case' safety factor (bending)	Peak calculated shear strain (με)	'Mean' safety factor (shear)	'Worst-case' safety factor (shear)
Iguana	Femur	1.45	+912	10.8	8.2	1625	4.9	4.3
	Tibia	1.05	+1733	5.7	3.6	*	*	*
Alligator	Femur	1.45	+1027	6.3	4.6	1489	5.4	3.4
	Tibia	3.00	+1173	5.5	3.9	2031	3.9	2.7

Peak strain estimates were calculated based on planar strain distributions; these provided a quantitative measure of the factorial increase in observed strains (Tables 1, 3) *versus* estimated peak strains.

Safety factors in bending were calculated using tensile yield strains measured in bending tests (9820 με for *Iguana*, 6495 με for *Alligator*, Table 5).

Safety factors in shear were calculated using a value of 8000 με for shear failure of vertebrate bone (Currey, 1984). 'Mean' and 'worst-case' safety factor calculations are described in the text.

*No rosette data were available for calculating shear strains in the iguana tibia.

comparisons of cross-sectional planar strain distributions for sprawling and upright steps at times of peak strain show that the femur consistently experiences relatively greater axial compression in more upright steps (Fig. 12; the neutral axis is displaced relatively further from the centroid).

Discussion

Locomotor loading of the femur and tibia in alligators and iguanas

Locomotor loading patterns of the hindlimb bones of alligators and iguanas are similar in many respects, but some key distinctions are also evident between these species, particularly in the tibia. Fig. 13 illustrates schematically the forces acting on an alligator femur and tibia during peak locomotor strain. In both alligators and iguanas, the femur experiences clockwise torsion (viewing the left femur from its proximal or distal end), dorsoventral bending (placing the dorsal cortex in compression and the ventral cortex in tension) and axial compression. In alligators, the tibia experiences counterclockwise torsion (viewing the left tibia from its proximal or distal end), anteroposterior bending (compression on the posterior surface, tension on the anterior surface) and axial compression. Although shear strains were not evaluated for the iguana tibia, the orientation of bending in the iguana tibia is similar to that in the alligator tibia (compression on the posterior surface, tension on the anterior surface). However, in contrast to results obtained for the alligator tibia, cross-sectional analyses of planar strain distributions for the iguana

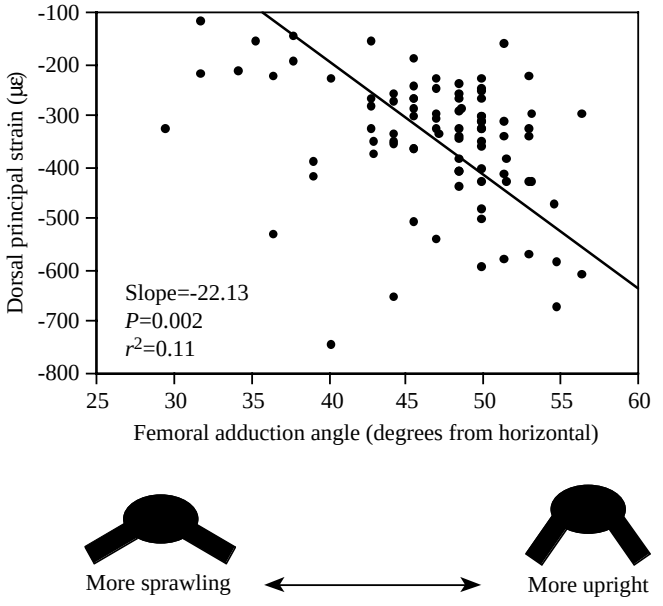

Fig. 11. Representative reduced major axis (RMA) regression of femoral strain magnitude on femoral adduction angle (alligator 1 dorsal principal compressive strain: see Table 7). More sprawling posture is to the left, more upright posture to the right (illustrated by schematic silhouettes below the graph).

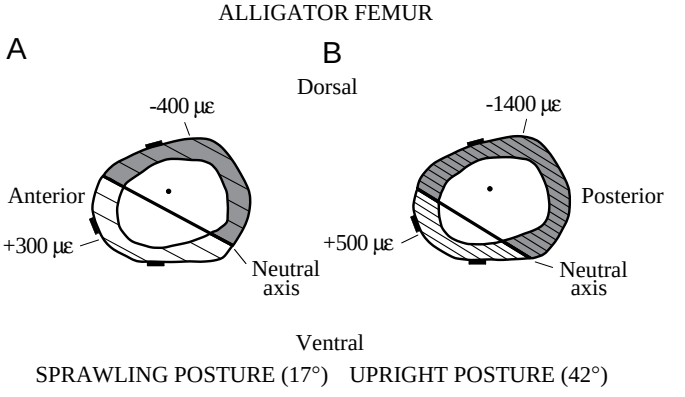

Fig. 12. Comparison of cross-sectional planar strain distributions at the time of peak strain for an alligator femur in sprawling (A) and upright (B) steps. For each cross section, the angular deviation of the femur from the horizontal is indicated in parentheses. Format and symbols as in Figs 8 and 9.

Table 7. *Summary of regressions of strain magnitude on femoral adduction angle (γ) for each recording location in each of the experimental alligators (larger angles indicate a more upright limb)*

Alligator	Recording site	Strain type	*N*	RMA slope	Change in absolute strain magnitude with more upright posture	r^2	*P*
1	Dorsal	Principal (compressive)	89	–22.13	Increase	0.11	0.002
		Shear	89	366.00	Increase	0.09	0.005
	Anterior	Longitudinal (tensile)	22	–15.20	Decrease	0.35	0.004
2	Dorsal	Principal (compressive)	34	NS	NS	NS	NS
		Shear	34	NS	NS	NS	NS
	Anterior	Longitudinal (tensile)	33	NS	NS	NS	NS
7	Dorsal	Principal (compressive)	67	–44.50	Increase	0.05	0.079*
		Shear	67	63.28	Increase	0.05	0.060*
	Ventral	Principal (tensile)	67	49.15	Increase	0.05	0.068*
		Shear	67	90.94	Increase	0.11	0.007
	Anterior	Longitudinal (tensile)	67	–23.51	Decrease	0.08	0.021

For changes in absolute strain magnitude with more upright posture, 'increase' in strain reflects greater deviation from zero strain at a recording site, and 'decrease' reflects strains closer to zero.

*Near-significant trends ($0.10>P>0.05$).

RMA, reduced major axis; *N*, number of steps; NS, not significant.

tibia consistently indicate net tension, rather than compression, at peak strain during walking and running. The prevalence of torsion of the femur and tibia of alligators and iguanas, as well as the presence of net tension of the iguana tibia, are unusual features that distinguish the limb bone loading patterns of these animals from those of most species in which limb bone strains during terrestrial locomotion have been examined.

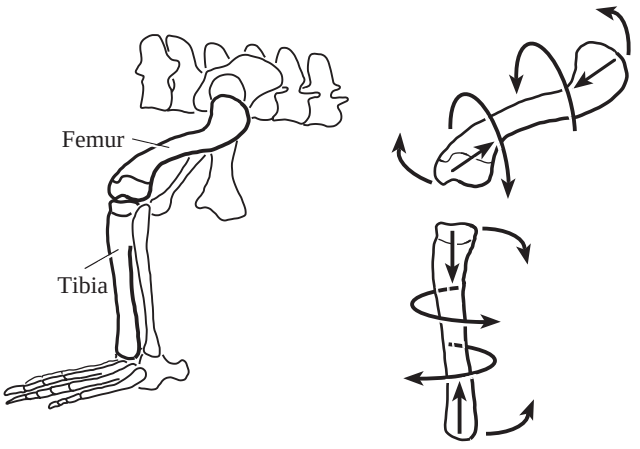

Fig. 13. Schematic illustration of loading in the alligator (*Alligator mississippiensis*) femur and tibia. Skeletal anatomy of the left hindlimb (lateral view) is shown on the left: the femur and tibia are highlighted with bold outlines. On the right, the bones are enlarged and separated at the knee, and arrows (not drawn to scale) indicate loading regimes inferred from *in vivo* strain recordings. Straight arrows indicate axial compression. Curved arrows at the ends of the elements indicate the compressive direction of bending. Arrows curving about bone diaphyses indicate the direction of torsion (clockwise for the left femur viewed proximally or distally, counterclockwise for the left tibia viewed proximally or distally).

Torsion is the dominant loading regime of the femur and tibia of alligators and the femur of iguanas (excepting the atypical strain patterns of iguana B). Deviations of principal strains from the long axes of these bones are substantial (ϕ_t=29–49 °), and peak shear strains exceed peak axial and bending strains by 45–78 %. Comparable magnitudes of shear strain due to torsion have been reported in the wing bones of bats and birds during flight (Swartz et al., 1992; Biewener and Dial, 1995), but few previous studies of *in vivo* limb bone strain during terrestrial locomotion have found torsion to be the most important mode of bone loading. Shear strains induced by torsion have been found to predominate in the femora of rats (Keller and Spengler, 1989) and chickens (Carrano, 1998), and moderate torsion (ϕ_t=25–30 °) has been reported for the tibia of sheep (Lanyon and Bourn, 1979) and the tibiotarsus of chickens (Biewener et al., 1986). However, most studies of terrestrial locomotion in mammals (e.g. Lanyon and Smith, 1970; Goodship et al., 1979; Rubin and Lanyon, 1982; Biewener et al., 1983, 1988; Biewener and Taylor, 1986) and birds (Rubin and Lanyon, 1984; Biewener et al., 1986; Biewener and Bertram, 1993) have found the limb bones to be loaded primarily in bending or occasionally in axial compression (e.g. horse metapodials; Biewener et al., 1983, 1988). The basic uniformity of these limb bone loading patterns is not entirely surprising, since most limb bone strain data have been collected from a phylogenetically limited set of species that move their limbs in parasagittal or nearly parasagittal planes (e.g. ungulate and carnivoran mammals, galliform birds). In contrast to the species examined in most previous studies, neither the lizard nor the crocodilian species examined in the present study employs strictly parasagittal hindlimb kinematics (Brinkman, 1980a, 1981; Gatesy, 1991a; Reilly and Elias, 1998). In addition, cineradiographic data

show that, in both alligators and iguanas, the femur and tibia undergo considerable axial rotation (Brinkman, 1980a, 1981; Gatesy, 1991a). These kinematic observations suggested the potential for the limb bones of iguanas and alligators to experience substantial torsion, as well as bending and axial loads – predictions borne out by our measurements of bone strain. The basic kinematic similarities among many lizard and crocodilian species (Snyder, 1952; Sukhanov, 1974; Brinkman, 1980b, 1981; Gatesy, 1991a; Reilly and DeLancey, 1997a,b) further suggest that the limb bone torsion observed for iguanas and alligators could generally characterize their respective lineages, although *in vivo* strains must be measured from the limb bones of more species to evaluate this possibility. Strain data from a greater kinematic and phylogenetic diversity of animals, particularly from unsampled lineages such as salamanders, turtles and marsupials (especially non-saltatory species), would help to determine whether torsion is a more common mode of limb bone loading during terrestrial locomotion than had been recognized on the basis of the initial data from mammals and birds. Strain data from a broader phylogenetic sample of species could also help to establish the extent to which observed instances of limb bone torsion might be retentions of ancestral traits or derived features of particular lineages.

The axial tension observed in the iguana tibia not only differs from the axial compression observed in the alligator tibia, but is unusual among vertebrate limb bones in general. Net axial tension has been reported during non-terrestrial locomotion for the humerus and ulna of brachiating gibbons (Swartz et al., 1989), for the humerus of flying bats (Swartz et al., 1992) and for the initial portion of the downstroke in flying pigeons (Biewener and Dial, 1995). However, in contrast to suspensory locomotion and flight, axial tension is unexpected in limb bones during terrestrial locomotion because the limbs are positioned beneath the body to support it above the substratum, against gravity. As a result, external forces acting on the limb (the ground reaction force and body weight) tend to compress the limb skeleton, supplementing internally transmitted compressive forces exerted by contracting muscles (Swartz et al., 1989).

Two factors that could contribute to net tension in the iguana tibia are the distinctive kinematics and robust fibula of iguanas compared with those of most species for which *in vivo* limb bone strains have been measured. In contrast to previously studied mammals and birds, iguanas orient the crus with the long axis nearly parallel to the ground for much of the support phase, including periods of peak strain (Fig. 14A). Kinematic analyses (R. W. Blob and A. A. Biewener, unpublished results) show that iguanas orient the crus at an angle of more than 70 ° from vertical for a mean of 66±6 % (mean ± S.D., N=15) of step duration, consistent with the observations of Brinkman (1981; his Fig. 3). In such an orientation, the entire crus would be subject to dorsoventral bending (in an absolute frame of reference), probably placing the dorsal aspect of the iguana crus in compression and the ventral aspect in tension. Although the tibia is initially positioned medial to the fibula (in an absolute frame of reference), lateral rotation of the crus during the step causes the tibia to shift ventrally and the fibula to shift dorsally. Because the fibula is robust relative to the tibia in iguanas, the net centroid for the bones of the crus is located

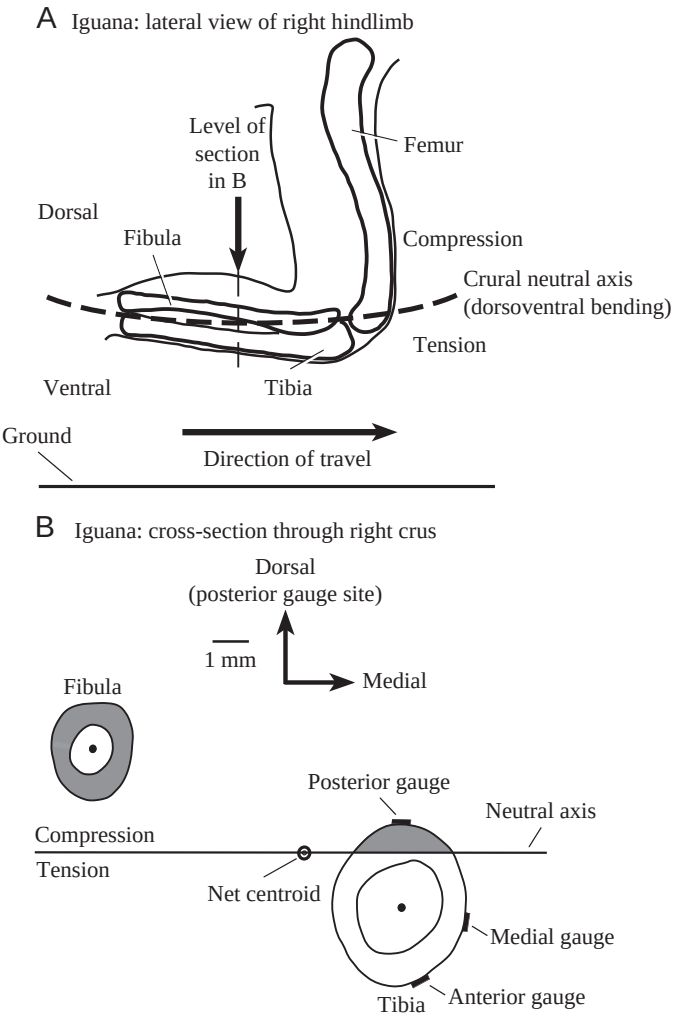

Fig. 14. Model for net tensile loading of the tibia in *Iguana iguana*. (A) Outline of the hindlimb and leg bones (right lateral view), drawn from a still radiograph. Direction of travel is to the right. The hindlimb is illustrated at a time during a step when the crus is oriented approximately parallel to the ground. In this position, the crus as a whole could be subject to dorsoventral bending (in an absolute frame of reference). Because the crural bones rotate during the step, the tibia shifts to a position ventral to the fibula. This could place the tibia largely on the tensile side of the neutral axis of dorsoventral bending in the crus. (B) Midshaft cross-section through the tibia and fibula of an iguana (*Iguana iguana*) illustrating the position of the centroid and the distribution of tensile (unshaded) and compressive (shaded) strains. The level of the section is indicated by the vertical arrow in A. Solid bars on the cortex of the tibia indicate strain gauge recording locations: note that the posterior recording site is oriented dorsally in an absolute frame of reference. The presence of the fibula displaces the net centroid of the lower leg bones to a position between the tibia and fibula, away from the centroid of the tibia. As a result, a larger portion of the tibia is located on the tensile side of the neutral axis than on the compressive side.

between them; thus, even if the crus as a whole experiences axial compression, the tibia can experience net tension because its cross section is positioned primarily on the tensile side of the crural neutral axis of bending (Fig. 14A,B). Other lizard species also appear to orient the tibia nearly horizontally for much of the support phase (e.g. *Sceloporus clarkii*; Reilly and DeLancey, 1997a,b) and, thus, might also experience tibial strain patterns similar to those observed for iguanas. In contrast to the iguana tibia, the alligator tibia exhibits the expected pattern of net axial compression. However, the tibia does not appear to be oriented horizontally for as substantial a portion of step duration in alligators (Gatesy, 1991a) as in iguanas. Furthermore, the tibia of *Alligator* is relatively more robust than that of *Iguana* (compare Figs 8B and 9), which would reduce the extent to which the crural centroid and neutral axis of bending are displaced from the tibia. Direct strain recordings from the fibula of both lizards and crocodilians would be useful to verify the loading regime of this element and its potential effects on the distribution of loads in the tibia of these species. Even though tension is an unusual loading regime for limb bones during terrestrial locomotion and bone is generally approximately 25 % weaker in tension than in compression (Currey, 1984), the iguana tibia would still be most likely to fail due to torsion if shear strains in the iguana tibia are as high (and torsional safety factors as low) as those observed in the alligator tibia.

Limb bone safety factors in Iguana *and* Alligator*: mechanical basis and evolutionary implications*

Safety factors for the femur and tibia of alligators and iguanas are generally higher than those previously reported for mammals and birds. ‘Mean’ safety factors to yield in bending for these two bones range from 5.5 to 10.8, considerably higher than previous calculations for mammals and birds based on recorded bone strains, which have varied between 1.4 and 4.3 (Lanyon and Rubin, 1985; Biewener, 1990, 1993). However, the high shear strains observed in *Alligator* and *Iguana* indicate that the limb bones of these animals face a greater risk of failure by torsion: safety factors for shear failure range between 3.9 and 5.4 (Table 6). Although lower than safety factors calculated on the basis of bending strains, these values are substantially higher than those reported for other limb bones subjected to considerable shear (e.g. 1.9 for the pigeon humerus during flight; Biewener and Dial, 1995). Furthermore, safety factors for shear failure in alligator and iguana limb bones appear at least moderately high compared with safety factors for vertebrate limb bones in general. A non-parametric, one-sample sign test comparing a sample of safety factors to yield for the limb bones of terrestrial mammals and birds (2.9±0.8; N=14, mean ± S.D.) with the lowest ‘mean’ shear-based safety factor for alligators or iguanas (3.9) gives a significant difference (P=0.002; mammalian and avian safety factor data compiled from Lanyon and Rubin, 1985; Biewener, 1993). Only the ‘worst-case’ safety factor estimates for alligator and iguana limb bones show substantial overlap with mammalian and avian values.

Limb bone safety factors depend upon two proximate factors: the magnitudes of forces acting on the bones and the mechanical properties of the bones. Differences in both of these factors between alligators and iguanas, on the one hand, and mammals and birds, on the other, appear to contribute to the differences in limb bone safety factors observed between these groups. The magnitudes of peak ground reaction force acting on the limbs, relative to body weight (W_b), are lower in iguanas and alligators than in birds and mammals. Force-platform recordings indicate that peak ground reaction force magnitudes acting on a single limb range between 1.3 and $2.4W_b$ for quadrupedal mammals in fast trots or gallops and can exceed $3W_b$ in running bipedal birds (Cavagna et al., 1977; Biewener, 1983a), but average only $1.1W_b$ in iguanas and $0.5W_b$ in alligators (Blob, 1998; R. W. Blob and A. A. Biewener, in preparation). Low ground reaction force magnitudes for *Alligator* are correlated with high duty factors, which decrease peak forces by increasing the time over which force is exerted on the limb (Alexander, 1977b; Biewener, 1983a,b). During fast locomotion ($0.37\,m\,s^{-1}$), hind foot duty factors for *Alligator* averaged 0.62±0.06 (N=173); in contrast, hind foot duty factors for *Iguana* averaged 0.44±0.03 (N=48) during running steps (Blob, 1998; R. W. Blob and A. A. Biewener, in preparation), similar to the values obtained for a broad size range of mammals at their trot–gallop transition (0.42±0.03; Biewener, 1983b).

Differences in the mechanical properties of the limb bones of alligators, iguanas, birds and mammals also appear to contribute to the differences in limb bone safety factor among these lineages, at least with respect to failure in bending. Tensile yield strains in bending for the limb bones of *Alligator* (+6495 με) and particularly *Iguana* (+9820 με) are higher than previously reported values for mammals and birds (+5250 με to +6000 με in tension, based on data from Currey, 1984; Biewener, 1993). These evaluations of yield strain for the limb bones of *Alligator* and *Iguana* appear conservative in the context of limited previous data on the mechanical properties of crocodilian and lizard limb bones. The high yield strain obtained for iguana limb bones is consistent with the relatively high tensile yield stresses (218–318 MPa) reported by Peterson and Zernicke (1987) for *Dipsosaurus dorsalis*, a closely related iguanian lizard (Norell and de Queiroz, 1991). Furthermore, Currey (1990) found a higher failure strain for the alligator femur (+21 000 με) than that measured in the present study (+13 366 με), although he did not report yield strain values. Because data for shear failure specific to alligator and iguana limb bones are not available, a general value for the failure strain of bone in shear (8000 με: Currey, 1984) was used in safety factor calculations. However, given the disparities in tensile yield strains observed among lizards, crocodilians, birds and mammals, it seems possible that differences in resistance to shear may also contribute to differences in the limb bone safety factors of these lineages.

Limb bone safety factor data are available for only a limited number of taxa, but the values calculated for *Iguana* and *Alligator* represent a starting point from which analyses of the

evolution of limb bone safety factor throughout amniotes can eventually proceed. The higher safety factors found for the hindlimb bones of *Iguana* and *Alligator* indicate the potential for an unexplored lack of uniformity in amniote limb bone safety factors, suggesting that the evolutionary history of limb bone mechanical design might be more complex than recognized previously. For instance, if safety factors in the limb bones of *Iguana* and *Alligator* were representative of the broader diversity of taxa within their respective lineages, then birds and mammals might not have inherited their similar safety factors from a common ancestor, but rather have evolved lower limb bone safety factors independently. To test this hypothesis, additional species of lepidosaurs and crocodilians must be sampled before the general patterns of limb bone strains and safety factors in these clades can be evaluated. Only single species from these clades were examined in the present study, and individuals from both species were subadults; thus, bone strains must be measured from other species and ages of lizards and crocodilians to establish whether the patterns found for *Iguana* and *Alligator* are generally true of their respective lineages. In addition, to evaluate the ancestral limb bone safety factor of amniotes and permit the distribution of character states for this trait to be assessed throughout amniote phylogeny, safety factors must be determined for the limb bones of species belonging to clades that are outgroups to Sauria (e.g. turtles) and to Amniota (e.g. salamanders and frogs). Until such data are collected, evolutionary hypotheses suggested by strain data and safety factor calculations from *Iguana* and *Alligator* must be viewed as preliminary and interpreted with caution.

If the relatively high safety factors observed in *Alligator* and *Iguana* are characteristic of lizards and crocodilians in general, why might the limb bones of these taxa be ‘overdesigned’ to a greater degree than those of other amniotes? Natural selection is often viewed as a primary factor regulating the magnitudes of biological safety factors, tending to eliminate safety factors that are too low to prevent regular failure of structures, or that are too high in terms of the cost of energy or space necessary for their maintenance (Alexander, 1981; Lanyon, 1991; Diamond and Hammond, 1992; Diamond, 1998). However, the degree to which natural selection acts to maintain biological safety factors of ‘optimum’ magnitude has been disputed (Garland, 1998). According to this view, the higher limb bone safety factors of *Alligator* and *Iguana* might represent retentions of the ancestral amniote or tetrapod condition that have not proved sufficiently disadvantageous to be selected against over time. Whether excessive safety factors could be maintained through hundreds of millions of years of evolution is questionable. To test this possibility, bone strain measurements and safety factor calculations will be required for taxa from additional amniote outgroups and from additional lizards and crocodilians.

It is also possible that the high limb bone safety factors observed in *Alligator* and *Iguana* are a consequence of a correlated response to selection on other phenotypic traits, rather than direct selection on safety factor itself (Lande and Arnold, 1983). Developmental covariation between the limb bones and other traits subjected to selection could produce limb bones in these species that incidentally have high safety factors. Across the range of safety factors between those exhibited by alligators and iguanas and those exhibited by mammals and birds, differences in selective costs for lower safety factors, in terms of decreased resistance to bone failure, and for higher safety factors, in terms of increases in the energy required to transport and maintain the limb bones, might not be large enough to override patterns of developmental covariation. Data documenting changes in the distribution of limb bone safety factors and other potentially correlated traits through generations of iguanas and alligators would be required to evaluate this possibility.

Despite these caveats, several factors could favor higher limb bone safety factors among alligators and iguanas and potentially contribute to selection against lower safety factors. For instance, although temperature, diet and exercise can all affect rates of bone remodeling in ‘reptiles,’ crocodilians and lizards have generally been found to remodel their bones at lower rates than birds and mammals (e.g. Enlow, 1969; de Ricqlès, 1975; Currey, 1984; de Ricqlès et al., 1991; Owerkowicz and Crompton, 1997). One function ascribed to bone remodeling is repair of accumulated microdamage (Lanyon et al., 1982; Currey, 1984; Burr et al., 1985). Low rates of bone remodeling in crocodilians and lizards could reflect a low incidence of microdamage in these lineages, a low capacity for microdamage repair or perhaps both. If microdamage repair capacities were limited by low rates of bone remodeling in alligators and iguanas, but the incidence of microdamage in their limb bones were as high as in the limb bones of other tetrapods, then low limb bone safety factors could be disadvantageous because they might be correlated with a greater possibility of limb bone failure due to fatigue (Carter et al., 1981).

The high limb bone safety factors of alligators and iguanas might also be correlated with greater variability of their locomotor loads or the mechanical properties of their skeletons, relative to the variability found in birds or mammals. Alexander (1981) has argued that increased variability of either the loads imposed on a biological structure or the mechanical properties of that structure should lead to selection for higher safety factors. Lowell (1985) observed patterns consistent with these predictions in populations of intertidal Pacific limpets, finding higher safety factors among animals from populations with higher variance in shell strength. Similar data are unavailable for vertebrate skeletal structures; however, such selective pressures might also have contributed to the evolution of relatively high safety factors in the limb bones of alligators and iguanas. Peak strain magnitudes appear to vary much more in alligators and iguanas than in the mammal or bird species examined previously. Coefficients of variation for peak strain magnitudes for series of steps at the same speed are typically 8 % or less in mammals and birds (Biewener, 1991), but range between 14 % and 50 % during fast locomotion in iguanas (Table 3) and between 37 % and 80 % during fast locomotion

in alligators (Table 1). In addition, the different strain patterns observed during fast locomotion in iguanas B and D (Figs 4, 5) suggest that marked interindividual differences in loading pattern, as well variation in load magnitudes, are possible in the locomotion of iguanas.

Bone strength also shows variability in crocodilians. Female alligators resorb endosteal structural bone from the femur during egg-laying, probably for use as a source of calcium for the formation of eggshells (Wink and Elsey, 1986). Such periodic bone resorption could lead to fluctuation in the mechanical strength of the femur, at least in females. Femoral bone resorption associated with egg-laying has also been identified in turtles (Edgren, 1960; Suzuki, 1963), suggesting that it may represent a plesiomorphic feature of amniotes and, therefore, might also occur in lizards. These observations suggest the potential for a combination of highly variable loading and bone material properties in crocodilians and lizards that may have favored the evolution of higher limb bone safety factors.

Femoral safety factors appear to be higher than those for the tibia among iguanas and alligators (Table 6). These results are consistent with the data of Currey (1984), who found the distal limb bones of horses to display fatigue fractures with greater frequency than the proximal limb bones, suggesting that the distal bones had lower safety factors. Currey (1984) argued that this pattern was related to the relatively greater contribution of distal mass to the moment of inertia of the leg and, therefore, to the energetic cost of moving the limb: selective pressure to reduce energetic costs would be expected to lead to decreased bone mass (and safety factors) distally. Alexander (1997, 1998) extended Currey's (1984) argument, mathematically demonstrating that, if probabilities of failure for all components of a linked system such as the limb skeleton are not perfectly correlated, then for a given total energetic cost the system would have a lower overall probability of failure if safety factors were greater in less energetically costly components (e.g. proximal limb bones) and lower in more energetically costly components (e.g. distal limb bones), rather than if safety factors were equal throughout the system. Alternatively, it is also possible that the difference in safety factors between proximal and distal limb bones in alligators and iguanas is a mechanical consequence of the torsional loading of their limb bones, rather than the product of selection against high safety factors that are energetically expensive to maintain. Because greater freedom of rotation is possible at the hip compared with either the knee or the ankle in lizards and crocodilians (Brinkman, 1980a,b; Rewcastle, 1980, 1983), less deformation (i.e. lower strains) might be produced in bones articulating in joints with low resistance to rotational motion (such as the femur), even without natural selection for distal decreases in bone mass.

Correlations between posture and strain in individual alligators: implications for the evolution of non-sprawling limb posture

Correlations between strain magnitudes and limb posture observed in *Alligator* are counterintuitive. Biewener (1989, 1990) has shown that a size-related shift from a crouched to an upright posture among mammals helps to maintain nearly constant limb bone stresses as body size increases. This postural shift aligns the limbs more closely with the ground reaction force vector, reducing external bending and the compressive muscular forces required to counter joint moments and maintain equilibrium. Although patterns of change can differ among hierarchical levels of organization (e.g. individuals relative to species: Gould, 1971), this previous work might predict fairly uniform decreases in strain levels for the limb bones of individual animals during a shift from a sprawling to an upright posture and consequent closer alignment of the limbs with the ground reaction force. Instead, our data show that the femoral cortex does not exhibit uniform changes in strain as posture shifts from sprawling to upright in *Alligator*: whereas tensile strains on the anterior cortex decrease with the use of a more upright posture, principal tensile and compressive strains on the dorsal and ventral cortices, as well as shear strains, frequently show significant increases (Table 7). These patterns of posture-related changes in strain magnitudes in alligators are consistent with patterns of posture-related changes in limb bone stresses during locomotion in green iguanas (determined from force-platform/kinematic data: Blob, 1998; R. W. Blob and A. A. Biewener, in preparation).

The observed pattern of changes in strain with changes in posture in alligators could be related to two factors. First, comparisons of cross-sectional planar strain distributions for sprawling and upright steps at times of peak strain show that in more upright steps the femur experiences relatively greater axial compression (Fig. 12; the neutral axis is displaced relatively further from the centroid of the bone cross section). This could reflect greater compressive loads induced during body support in upright posture, which would tend to reduce tensile strains due to bending on the anterior and ventral cortices. Second, analyses of force platform data from iguanas suggest that increases in stress (or strain) on the dorsal and ventral cortices of the femur are correlated with increases in the force exerted by the knee extensor muscles as limb posture becomes more upright, with the increases in muscle force resulting from increased moments at the ankle and knee (Blob, 1998; R. W. Blob and A. A. Biewener, in preparation). Given the similarity in posture-related changes in loading observed between *Alligator* and *Iguana* (Blob, 1998), it seems likely that a similar mechanism of changes in muscle forces could account for the posture-related changes in limb bone loading observed in both species.

What are the implications of these observations for the interpretation of evolutionary shifts in limb posture? Limits to acceptable (i.e. safe) levels of limb bone strain have probably placed some boundaries on the diversity of locomotor morphology and terrestrial kinematics that have evolved in tetrapods. However, shifts from a sprawling to an upright posture within alligators appear insufficient to cause substantial reductions in limb bone strain. Therefore, it is

possible that shifts in posture would have been similarly ineffectual as a means of reducing limb bone strain through evolutionary transitions from a sprawling to an upright stance. For example, shear strains appear to increase during upright locomotion in *Alligator*. Reduction of shear, which represents the most substantial strain experienced by the lizard and crocodilian species observed in this study, probably requires a shift to predominantly parasagittal limb kinematics and a reduction in axial rotation of the femur, not just an upright posture.

It is possible that limb bone strain might not have been maintained at similar magnitudes throughout the evolution of more upright posture in some lineages: for instance, the data from *Alligator* suggest that limb bone stresses and strains could increase through evolutionary transitions to an upright posture. However, in some lineages, an evolutionary decrease in size may have helped to mitigate posture-related increases in loads. Neglecting possible allometric effects, as body size in a lineage decreases, the loads limb bones must resist will decrease in proportion to the cube of mass, but the resistance of limb bones to loads (correlated with bone cross-sectional area) will decrease only in proportion to the square of mass, leading to relatively greater resistance to loads in the limb bones of smaller taxa. One postural transition that may have been subject to such effects is the evolution of non-sprawling posture in therapsids (derived 'mammal-like reptiles'). In the locomotor evolution of therapsids, characters associated with upright posture (e.g. changes in pelvic and femoral morphology) are gradually acquired throughout the transition from gorgonopsians to basal mammals, but early mammals are considerably smaller than non-mammalian therapsids (Jenkins, 1971b; Jenkins and Parrington, 1976; Kemp, 1982, 1985; Hopson, 1991, 1994; Sidor and Hopson, 1998). This evolutionary decrease in size (and consequent relatively greater resistance to limb bone loads) might have helped to counter posture-related increases in limb bone strain and decreases in limb bone safety factor through the 'reptile'-to-mammal transition.

The strain data collected in this study indicate that evolutionary transitions from sprawling to non-sprawling posture within a clade cannot be treated as directly analogous to size-correlated evolutionary transitions from a crouched to an upright posture, such as those seen in mammals that employ predominantly parasagittal limb kinematics. In species that use non-parasagittal kinematics, the use of a more upright posture could increase bone strains, rather than reduce them. Large increases in size within sprawling lineages might place restrictions on locomotor behavior similar to those seen among larger mammals (Biewener, 1990), a possibility that remains to be tested. However, without scale-dependent increases in loading associated with increases in size, posture-related increases in bone strain might not be a critical limitation, particularly for species with high limb bone safety factors. Selection pressure to limit bone loads probably contributed to the evolution of some shifts in limb posture, but may not have been a factor common to all such transitions.

We greatly appreciate the critical comments and thoughtful advice of M. Carrano, B. Chernoff, W. Corning, N. Espinoza, S. Gatesy, J. Hopson, F. Jenkins Jr, D. Konieczynski, M. LaBarbera, P. Magwene, E. Maillet, L. Panko, S. Reilly, C. Sidor, J. Socha, M. Temaner, M. Westneat, J. Wilson, the University of Chicago Biomechanics Discussion Group and two anonymous referees. We are also grateful to R. Elsey (Rockefeller Wildlife Refuge) for generously providing the alligators used in this research, to B. Brand, D. Croft, J. Furneaux-Noor, J. Kohler and H. Larsson for assistance with data collection, to M. LaBarbera for access to the tensometer, to J. Gilpin for building the animal enclosure and machining the tensometer grips, to C. Abraczinskas for advice on figures and to J. Alipaz, J. Schwartz and S. Seps for help with animal care. This research was supported by the University of Chicago Hinds Fund (R.W.B.), the Society of Vertebrate Paleontology Predoctoral Fellowship (R.W.B.) and by NSF grants IBN-9520719 (R.W.B.), IBN-9306793 and IBN-9723699 (A.A.B.).

References

Alexander, R. McN. (1977a). Terrestrial locomotion. In *Mechanics and Energetics of Animal Locomotion* (ed. R. McN. Alexander and G. Goldspink), pp. 168–203. London: Chapman & Hall.

Alexander, R. McN. (1977b). Allometry of the limbs of antelopes (Bovidae). *J. Zool., Lond.* **183**, 125–146.

Alexander, R. McN. (1981). Factors of safety in the structure of animals. *Sci. Prog.* **67**, 109–130.

Alexander, R. McN. (1997). A theory of mixed chains applied to safety factors in biological systems. *J. Theor. Biol.* **184**, 247–252.

Alexander, R. McN. (1998). Symmorphosis and safety factors. In *Principles of Animal Design: the Optimization and Symmorphosis Debate* (ed. E. W. Weibel, C. R. Taylor and L. Bolis), pp. 28–35. Cambridge: Cambridge University Press.

Bennett, R. A. (1991). A review of anesthesia and chemical restraint in reptiles. *J. Zoo Wildl. Med.* **22**, 282–303.

Bertram, J. E. A. and Biewener, A. A. (1990). Differential scaling of the long bones in the terrestrial Carnivora and other mammals. *J. Morph.* **204**, 157–169.

Biewener, A. A. (1983a). Locomotory stresses in the limb bones of two small mammals: the ground squirrel and chipmunk. *J. Exp. Biol.* **103**, 131–154.

Biewener, A. A. (1983b). Allometry of quadrupedal locomotion: the scaling of duty factor, bone curvature and limb orientation to body size. *J. Exp. Biol.* **105**, 147–171.

Biewener, A. A. (1989). Scaling body support in mammals: limb posture and muscle mechanics. *Science* **245**, 45–48.

Biewener, A. A. (1990). Biomechanics of mammalian terrestrial locomotion. *Science* **250**, 1097–1103.

Biewener, A. A. (1991). Musculoskeletal design in relation to body size. *J. Biomech.* **24** (Suppl. 1), 19–29.

Biewener, A. A. (1992). *In vivo* measurement of bone strain and tendon force. In *Biomechanics – Structures and Systems: A Practical Approach* (ed. A. A. Biewener), pp. 123–147. New York: Oxford University Press.

Biewener, A. A. (1993). Safety factors in bone strength. *Calcif. Tissue Int.* **53** (Suppl. 1), S68–S74.

Biewener, A. A. and Bertram, J. E. A. (1993). Skeletal strain

patterns in relation to exercise training during growth. *J. Exp. Biol.* **185**, 51–69.

Biewener, A. A. and Dial, K. P. (1995). *In vivo* strain in the humerus of pigeons (*Columba livia*) during flight. *J. Morph.* **225**, 61–75.

Biewener, A. A., Swartz, S. M. and Bertram, J. E. A. (1986). Bone modeling during growth: dynamic strain equilibrium in the chick tibiotarsus. *Calcif. Tissue Int.* **39**, 390–395.

Biewener, A. A. and Taylor, C. R. (1986). Bone strain: a determinant of gait and speed. *J. Exp. Biol.* **123**, 383–400.

Biewener, A. A., Thomason, J., Goodship, A. and Lanyon, L. E. (1983). Bone stress in the horse forelimb during locomotion at different gaits: a comparison of two experimental methods. *J. Biomech.* **16**, 565–576.

Biewener, A. A., Thomason, J. and Lanyon, L. E. (1988). Mechanics of locomotion and jumping in the horse (*Equus*): *in vivo* stress in the tibia and metatarsus. *J. Zool., Lond.* **214**, 547–565.

Blob, R. W. (1998). Mechanics of non-parasagittal locomotion in *Alligator* and *Iguana*: functional implications for the evolution of non-sprawling posture in the Therapsida. PhD dissertation, University of Chicago, Chicago.

Boyer, T. H. (1992). Clinical anesthesia of reptiles. *Bull. Ass. Rept. Amphib. Vet.* **2**, 10–13.

Brinkman, D. (1980a). Structural correlates of tarsal and metatarsal functioning in *Iguana* (Lacertilia; Iguanidae) and other lizards. *Can. J. Zool.* **58**, 277–289.

Brinkman, D. (1980b). The hind limb step cycle of *Caiman sclerops* and the mechanics of the crocodile tarsus and metatarsus. *Can. J. Zool.* **58**, 2187–2200.

Brinkman, D. (1981). The hind limb step cycle of *Iguana* and primitive reptiles. *J. Zool., Lond.* **181**, 91–103.

Brochu, C. A. (1997). Morphology, fossils, divergence timing and the phylogenetic relationships of *Gavialis*. *Syst. Biol.* **46**, 479–522.

Burr, D. B., Martin, R. B., Schaffler, M. B. and Radin, E. L. (1985). Bone remodeling in response to *in vivo* fatigue microdamage. *J. Biomech.* **18**, 189–200.

Burstein, A. H., Currey, J. D., Frankel, V. H. and Reilly, D. T. (1972). The ultimate properties of bone tissue: the effects of yielding. *J. Biomech.* **5**, 35–44.

Carrano, M. T. (1998). The evolution of dinosaur locomotion: functional morphology, biomechanics and modern analogs. PhD dissertation, University of Chicago, Chicago.

Carter, D. R. (1978). Anisotropic analysis of strain rosette information from cortical bone. *J. Biomech.* **11**, 199–202.

Carter, D. R., Harris, W. H., Vasu, R. and Caler, W. E. (1981). The mechanical and biological response of cortical bone to *in vivo* strain histories. In *Mechanical Properties of Bone* (AMD vol. 45) (ed. S. C. Cowin), pp. 81–92. New York: American Society of Mechanical Engineers.

Cavagna, G. A., Heglund, N. C. and Taylor, C. R. (1977). Mechanical work in terrestrial locomotion: two basic mechanisms for minimizing energy expenditure. *Am. J. Physiol.* **233**, R243–R261.

Currey, J. D. (1984). *The Mechanical Adaptations of Bones*. Princeton, NJ: Princeton University Press.

Currey, J. D. (1990). Physical characteristics affecting the tensile failure properties of compact bone. *J. Biomech.* **23**, 837–844.

Currey, J. D. and Brear, K. (1974). Tensile yield in bone. *Calc. Tissue Res.* **15**, 173–179.

Dally, J. W. and Riley, W. F. (1978). *Experimental Strain Analysis*. New York: McGraw-Hill.

de Ricqlès, A. J. (1975). On bone histology of living and fossil reptiles, with comments on its functional and evolutionary significance. In *Morphology and Biology of Reptiles* (ed. A. d'A. Bellairs and C. B. Cox), pp. 123–150. Linnean Society Symposium Series, Number 3.

de Ricqlès, A. J., Meunier, F. J., Castanet, J. and Francillon-Vieillot, H. (1991). Comparative microstructure of bone. In *Bone*, vol. 3, *Bone Matrix and Bone Specific Products* (ed. B. K. Hall), pp. 1–78. Boca Raton, FL: CRC Press.

Diamond, J. M. (1998). Evolution of biological safety factors: a cost/benefit analysis. In *Principles of Animal Design: the Optimization and Symmorphosis Debate* (ed. E. W. Weibel, C. R. Taylor and L. Bolis), pp. 21–27. Cambridge: Cambridge University Press.

Diamond, J. and Hammond, K. (1992). The matches, achieved by natural selection, between biological capacities and their natural loads. *Experientia* **48**, 551–557.

Edgren, R. A. (1960). A seasonal change in bone density in female musk turtles, *Sternothaerus odoratus* (Latreille). *Comp. Biochem. Physiol.* **1**, 213–217.

Enlow, D. H. (1969). The bone of reptiles. In *Biology of the Reptilia*, I, *Morphology A* (ed. C. Gans, A. d'A. Bellairs and T. S. Parsons), pp. 45–80. London: Academic Press.

Frye, F. L. (1995). *Reptile Clinician's Handbook: A Compact Clinical and Surgical Reference*. Malabar, FL: Kreiger Publishing Company.

Garland, T., Jr (1998). Conceptual and methodological issues in testing the predictions of symmorphosis. In *Principles of Animal Design: the Optimization and Symmorphosis Debate* (ed. E. W. Weibel, C. R. Taylor and L. Bolis), pp. 40–47. Cambridge: Cambridge University Press.

Gatesy, S. M. (1991a). Hind limb movements of the American alligator (*Alligator mississippiensis*) and postural grades. *J. Zool., Lond.* **224**, 577–588.

Gatesy, S. M. (1991b). Hind limb scaling in birds and other theropods: implications for terrestrial locomotion. *J. Morph.* **209**, 83–96.

Gatesy, S. M. (1997). An electromyographic analysis of hindlimb function in *Alligator* during terrestrial locomotion. *J. Morph.* **234**, 197–212.

Gauthier, J., Kluge, A. G. and Rowe, T. (1988). The early evolution of the Amniota. In *The Phylogeny and Classification of the Tetrapods*, vol. 1 (ed. M. J. Benton), pp. 103–155. Oxford: Clarendon Press.

Goodship, A. E., Lanyon, L. E. and McFie, H. (1979). Functional adaptation of bone to increased stress. *J. Bone Jt Surg.* **61**A, 539–546.

Gould, S. J. (1971). Geometric scaling in allometric growth: a contribution to the problem of scaling in the evolution of size. *Am. Nat.* **105**, 113–136.

Hopson, J. A. (1991). Systematics of the nonmammalian Synapsida and implications for patterns of evolution in synapsids. In *Origins of the Higher Groups of Tetrapods: Controversy and Consensus* (ed. H.-P. Schultze and L. Trueb), pp. 635–693. Ithaca, London: Comstock Publishing Associates.

Hopson, J. A. (1994). Synapsid evolution and the radiation of non-eutherian mammals. In *Major Features of Vertebrate Evolution, Short Course in Paleontology*, vol. 7 (ed. D. R. Prothero and R. M. Schoch), pp. 190–219. Knoxville, KY: The Paleontological Society.

Jenkins, F. A., Jr (1971a). Limb posture and locomotion in the

Virginia opossum (*Didelphis marsupialis*) and in other non-cursorial mammals. *J. Zool., Lond.* **165**, 303–315.

Jenkins, F. A., Jr (1971b). The postcranial skeleton of African cynodonts. *Bull. Peabody Mus. Nat. Hist.* **36**, 1–216.

Jenkins, F. A., Jr and Parrington, F. R. (1976). The postcranial skeletons of the Triassic mammals *Eozostrodon*, *Megazostrodon* and *Erythrotherium*. *Phil. Trans. R. Soc. B* **273**, 387–431.

Keller, T. S. and Spengler, D. M. (1989). Regulation of bone stress and strain in the immature and mature rat femur. *J. Biomech.* **22**, 1115–1127.

Kemp, T. S. (1982). *Mammal-like Reptiles and the Origin of Mammals*. London: Academic Press.

Kemp, T. S. (1985). A functional interpretation of the transition from primitive tetrapod to mammalian locomotion. In *Principles of Construction in Fossil and Recent Reptiles* (ed. J. Reiß and E. Frey), pp. 181–191. Stuttgart: Universität Stuttgart/Universität Tübingen.

LaBarbera, M. (1989). Analyzing body size as a factor in ecology and evolution. *Annu. Rev. Ecol. Syst.* **20**, 97–117.

Lande, R. and Arnold, S. J. (1983). The measurement of selection on correlated characters. *Evolution* **37**, 1210–1226.

Lanyon, L. E. (1991). Biomechanical properties of bone and response of bone to mechanical stimuli: functional strain as a controlling influence on bone modeling and remodeling behavior. In *Bone*, vol. 3, *Bone Matrix and Bone Specific Products* (ed. B. K. Hall), pp. 79–108. Boca Raton, FL: CRC Press.

Lanyon, L. E. and Bourn, S. (1979). The influence of mechanical function on the development and remodeling of the tibia. *J. Bone Jt Surg.* **61**A, 263–273.

Lanyon, L. E., Goodship, A. E., Pye, C. J. and MacFie, J. H. (1982). Mechanically adaptive bone remodelling. *J. Biomech.* **15**, 141–154.

Lanyon, L. E. and Rubin, C. T. (1985). Functional adaptation in skeletal structures. In *Functional Vertebrate Morphology* (ed. M. Hildebrand, D. M. Bramble, K. F. Liem and D. B. Wake), pp. 1–25. Cambridge, MA: The Belknap Press.

Lanyon, L. E. and Smith, R. N. (1970). Bone strain in the tibia during normal quadrupedal locomotion. *Acta Orthoped. Scand.* **41**, 238–248.

Lowell, R. B. (1985). Selection for increased safety factors of biological structures as environmental unpredictability increases. *Science* **228**, 1009–1011.

Norell, M. A. and de Queiroz, K. (1991). The earliest iguanine lizard (Reptilia: Squamata) and its bearing on iguanine phylogeny. *Am. Mus. Nov.* **2997**, 1–16.

Owerkowicz, T. and Crompton, A. W. (1997). Effects of exercise and diet on bone-building: a monitor case. *J. Morph.* **232**, 306.

Peterson, J. A. and Zernicke, R. F. (1987). The geometric and mechanical properties of limb bones in the lizard, *Dipsosaurus dorsalis*. *J. Biomech.* **20**, 902.

Reilly, S. M. and DeLancey, M. J. (1997a). Sprawling locomotion in the lizard *Sceloporus clarkii*: quantitative kinematics of a walking trot. *J. Exp. Biol.* **200**, 753–765.

Reilly, S. M. and DeLancey, M. J. (1997b). Sprawling locomotion in the lizard *Sceloporus clarkii*: the effects of speed on gait, hindlimb kinematics and axial bending during walking. *J. Zool., Lond.* **243**, 417–433.

Reilly, S. M. and Elias, J. A. (1998). Locomotion in *Alligator mississippiensis*: kinematic effects of speed and posture and their relevance to the sprawling-to-erect paradigm. *J. Exp. Biol.* **201**, 2559–2574.

Rewcastle, S. C. (1980). Form and function in the lacertilian knee and mesotarsal joints; a contribution to the analysis of sprawling locomotion. *J. Zool., Lond.* **191**, 147–170.

Rewcastle, S. C. (1983). Fundamental adaptations in the lacertilian hindlimb: a partial analysis of the sprawling limb posture and gait. *Copeia* **1983**, 476–487.

Romer, A. S. (1956). *Osteology of the Reptiles*. Chicago: University of Chicago Press.

Rubin, C. T. and Lanyon, L. E. (1982). Limb mechanics as a function of speed and gait: a study of functional strains in the radius and tibia of horse and dog. *J. Exp. Biol.* **101**, 187–211.

Rubin, C. T. and Lanyon, L. E. (1984). Dynamic strain similarity in vertebrates: an alternative to allometric limb bone scaling. *J. Theor. Biol.* **107**, 321–327.

Sidor, C. A. and Hopson, J. A. (1998). Ghost lineages and 'mammalness': assessing the temporal pattern of character acquisition in the Synapsida. *Paleobiol.* **24**, 254–273.

Snyder, R. C. (1952). Quadrupedal and bipedal locomotion of lizards. *Copeia* **1952**, 64–70.

Snyder, R. C. (1962). Adaptations for bipedal locomotion of lizards. *Am. Zool.* **2**, 191–203.

Sokal, R. R. and Rohlf, F. J. (1995). *Biometry*, third edition. New York: W. H. Freeman & Company.

Sukhanov, V. B. (1974). *General System of Symmetrical Locomotion of Terrestrial Vertebrates and Some Features of Movement in Lower Tetrapods* (translated by M. M. Hague). New Dehli: Amerind Publishing Co. Pvt. Ltd.

Suzuki, H. K. (1963). Studies on the osseous system of the slider turtle. *Ann. N.Y. Acad. Sci.* **109**, 351–410.

Swartz, S. M., Bennett, M. B. and Carrier, D. R. (1992). Wing bone stresses in free flying bats and the evolution of skeletal design for flight. *Nature* **359**, 726–729.

Swartz, S. M., Bertram, J. E. A. and Biewener, A. A. (1989). Telemetered *in vivo* strain analysis of locomotor mechanics in brachiating gibbons. *Nature* **342**, 270–272.

Updegraff, G. (1990). *Measurement TV: Video Analysis Software*. San Clemente, CA: Data Crunch.

Wink, C. S. and Elsey, R. M. (1986). Changes in femoral morphology during egg-laying in *Alligator mississippiensis*. *J. Morph.* **189**, 183–188.